CANADA

DEPARTMENT OF
ENERGY, MINES AND RESOURCES
MINES BRANCH
OTTAWA

BEHAVIOUR OF THICK-WALL GALVANIZED PRODUCTS AT ELEVATED TEMPERATURES

J. J. SEBISTY AND R. H. PALMER

PHYSICAL METALLURGY DIVISION

DECEMBER 1968

Research Report R 200

Price $1.00

Available by mail from the Queen's Printer, Ottawa,
and at the following Canadian Government bookshops:

OTTAWA
Daly Building, Corner Mackenzie and Rideau

TORONTO
221 Yonge Street

MONTREAL
Æterna-Vie Building, 1182 St. Catherine St. West

WINNIPEG
Mall Center Building, 499 Portage Avenue

VANCOUVER
657 Granville Avenue

HALIFAX
1737 Barrington Street

or through your bookseller

A deposit copy of this publication is also available
for reference in public libraries across Canada

Price $1.00 Catalogue No. M38-1/200

Price subject to change without notice

Queen's Printer and Controller of Stationery
Ottawa, Canada
1969

Mines Branch Research Report R 200

BEHAVIOUR OF THICK-WALL GALVANIZED PRODUCTS AT ELEVATED TEMPERATURES

by

J. J. Sebisty* and R. H. Palmer*

- - - - - -

ABSTRACT

In this investigation, the elevated-temperature behaviour of hot-dip galvanized tubing, angle and bar products of Canadian and European origin was examined. Air-atmosphere heating tests were made in the temperature range of 200-400°C (390-750°F) for periods up to one year.

Galvanized coating deterioration was found to involve separation and gradual dissolution of the outer zinc layer, in combination with transformation changes in the underlying iron-zinc alloy layers. The deterioration process was mainly dependent on the time-temperature conditions of heating, but also was significantly influenced by the microstructural characteristics of the as-galvanized coating and the inherent chemical reactivity of the steel base. By virtue of a more favourable combination of these last two factors, one of the tubing products and one of the angle products were found to be somewhat superior at the industry-recommended limiting service temperature of 200°C (390°F).

---

*Research Scientists, Non-Ferrous Metals Section, Physical Metallurgy Division, Mines Branch, Department of Energy, Mines and Resources, Ottawa, Canada.

Direction des mines

Rapport de recherches R 200

COMPORTEMENT À TEMPÉRATURE ÉLEVÉE DES PRODUITS GALVANISÉS À PAROI ÉPAISSE

par

J. J. Sebisty* et R. H. Palmer*

RÉSUMÉ

Dans cette étude, les auteurs ont examiné le comportement à température élevée de tubages, cornières et barres d'origine candienne et européenne galvanisés par immersion à chaud. Des essais de chauffage (air-atmosphère) ont été faits à des températures variant entre 200° et 400° C (390° à 750°F) pendant des périodes allant jusqu'à un an.

Les auteurs ont trouvé que la détérioration du revêtement galvanisé s'accomplissait par la séparation et la dissolution progressive de la couche extérieure de zinc, accompagnées de transformations des couches sous-jacentes de l'alliage fer-zinc. Le processus de détérioration dépend principalement des conditions de chauffage durée-température mais les caractéristiques microstructurales du revêtement galvanisé et la réactivité chimique inhérente de la base d'acier y jouent également un rôle important. Grâce à une combinaison plus favorable de ces deux derniers facteurs, ils ont trouvé qu'un des tubages et une des cornières faisaient preuve de qualité quelque peu supérieure à la température d'usage maximale de 200°C (390°F) recommandée par le manufacturier.

---

* Chercheurs scientifiques, Section des métaux non-ferreux, Division de la métallurgie physique, Direction des mines, ministère de l'Energie, des Mines et des Ressources, Ottawa, Canada.

CONTENTS

TABLES

FIGURES

(Figures, concluded)

- - - - - - -

INTRODUCTION

The object of this investigation was to study the influence of long-term elevated-temperature heating on the behaviour of conventional galvanized coatings. Commercially coated tubing, angle and bar products of Canadian and European origin were selected, and heated in air in the temperature range 200°-400°C (390°-750°F) for periods up to one year. Evaluation of coating deterioration was based principally on changes in surface appearance, chemical composition and microstructure of the coatings. Data not previously available were accumulated, and information on the rate and mode of deterioration of conventional galvanized coatings heated at temperatures below the melting point of zinc was considerably expanded.

The investigation was carried out with the co-operation and support of the Canadian Zinc and Lead Research Committee (CZLRC) and the International Lead Zinc Research Organization, Inc. (ILZRO).

REVIEW OF PREVIOUS WORK

No published information is available on the long-term service performance of conventional galvanized coatings at elevated temperatures. Continuous-strip coatings were studied in a prior investigation[1][2], but these represent an entirely different class of coating, microstructurally and in other respects. Of relevance is Hershman's work[3] which examined the peeling that can occur when galvanized articles are slowly cooled, or are heated for short periods to temperatures below the melting point of zinc. He found that cavitation was developed at the zinc-zeta interface with short exposures at temperatures above 325°C (615°F). An undefined lower-temperature limit was suggested to avoid the effect with long-term exposure. In a discussion[4] on Hershman's paper, a temperature maximum of 200°C (390°F) for long service use was recommended. This was based on the

present work and other related studies[5], and on an industry-recommended service temperature limit for conventional coatings[6].

Various other scattered notes and reports[7-12] on the peeling problem may be found, all of which refer to the separation occurring immediately after galvanizing. Slow cooling is considered to be principally responsible, but both the surface condition of the steel and the difference in coefficient of expansion of zinc and iron are also mentioned as other probable factors.

MATERIALS

Procurement of the six materials for testing was arranged through ILZRO. These included 3/4-in. (1.9-cm), standard-weight, welded galvanized tubing of Canadian manufacture and two batches of similar-size tubing of European origin. One of the latter was seamless tubing (probably cold drawn); the other was a welded product. Hot-rolled galvanized angles from Canadian and European suppliers, and bar stock of Canadian manufacture, were also received.

Details provided on the pretreatment and galvanizing conditions for the six products are consolidated in Tables 1 and 2. The steel-base compositions as determined by the Mineral Sciences Division, Mines Branch, are given in Table 3.

All three tubing steels appeared to be rimming grades, although CT had been designated a capped steel. The welded products (CT and ET) had typical pearlitic structures, as shown in Figure 1. Evidence of cold working distinguished the seamless tubing (DT), as in Figure 1(b).

As is to be expected with tube-galvanizing practice, the inner coatings on the different tubes were generally markedly thicker than on the outside. This variation is usually related to the retention of a thicker zinc

layer on the steam-wiped inner surface. It was, however, also partly dependent on the steel-base roughness, and on the attendant non-uniformity in iron-zinc alloy growth which influenced zinc drag-out (Figure 2). Minimum roughness was observed with the seamless tubing (DT) and, as Figure 2(b) suggests, this was reflected in much better coating-thickness uniformity on the inner and outer surfaces of this product.

The steel-base microstructures for the angle and bar products are also shown in Figure 1. Angle DA was a rimming steel with a fine-grained ferrite structure, whereas Angle CA and Bar CB were both semi-killed and had fine-grained pearlitic structures. Both of the latter were in the silicon range where, according to Sandelin[13], accelerated galvanizing attack may occur. However, despite the similarity in steel-base composition and microstructure, as well as galvanizing preparation, Angle CA only was so affected. It had a very thick coating, made up largely of fine zeta crystals embedded in a zinc matrix (Figure 3(b)). Bar CB showed a more conventional layered-structure of iron-zinc alloy, as in Figure 3(c). It can only be assumed that the steel surface condition, as affected by processing history, in some way favoured accelerated attack of Angle CA but not of Bar CB.

The chemical compositions of the coatings on the six products are listed in Table 4. Conventional zinc-lead compositions are indicated, with copper impurities present in some cases and tin in others. In so far as surface appearance was concerned, all the coatings were bright, and varied from a metallic to a lightly-spangled finish. Spangling was more prominent on Tubing DT and Angle DA, possibly because of the presence of tin in the coating.

EXPERIMENTAL PROGRAM

The purpose of the investigation was to evaluate and compare the performance of the six products when exposed to an air-atmosphere environment over a range of time-temperature conditions. To this end, the experimental test program defined in Table 5 was carried out.

In the tests at 200°C (390°F), 250°C (480°F) and 300°C (570°F), samples 6 in. (15 cm) long of Tubings CT, DT, ET and Angle DA were heated for exposure periods varying from 4 hours up to 24 weeks. One additional sample of each of these materials was exposed at 200°C (390°F) for 1 year, and a sample of Tubing CT was heated for the same period at 250°C (480°F). Supplies of Angle CA and Bar CB were received late in the program, and tests on these were restricted to exposure at 250°C (480°F) and 300°C (570°F).

The program also involved some preliminary experiments in which Tubing CT was heated at 400°C (750°F) for periods of from 1/2 hour to 4 weeks. The main purpose was to determine the need for inclusion of mechanical testing in the lower-temperature tests which followed. Secondly, it was hoped to obtain metallographic information on high reaction-rate effects which could aid in interpretation and evaluation of the results at the lower temperatures.

The influence of heating was evaluated by surface inspection, coating-weight and iron-content determinations, metallographic examination, and, in some cases as described later, by bend and tensile tests (Table 6) on the steel base. Uninhibited 20% HCl acid solution was used for the stripping tests, thereby simplifying the titration for iron. Only one surface was stripped at a time, so as to eliminate the effect of coating-thickness variations (particularly inherent with the tubing products). Metallographic etchants based on those developed by Rowland[14] were used to reproduce microstructural effects. For the tensile tests, half-section pieces

7 in. (17.5 cm) long were machined to the required gauge length and then flattened at each end to facilitate gripping.

The averaged results of the quantitative coating-weight and iron-content stripping tests are given in Tables 7 to 12. As in the prior work on strip coatings[1][2], only the iron-content determinations provided a meaningful measure of reaction-rate effects, and these are graphed in Figures 4 to 7. Typical coating microstructures are shown in Figures 8 to 18. For convenience in discussion, the tubing products, and the angle and bar materials, are treated separately in that order.

RESULTS FOR TUBING PRODUCTS

Surface Effects

Oxidation was the only exterior surface change on Tubing CT after heating for up to 12 weeks at 200°C (390°F). At longer exposures, from 16 to 24 weeks, local thinning and disappearance of the outer zinc layer occurred, leaving numerous dark patches of the underlying zeta phase exposed. Zinc remaining at this stage did not appear to lose its adherence, presumably because of mechanical keying. Similar iron-zinc alloy penetration through the surface was evident on Tubing ET at 24 weeks, but Tubing DT was relatively unaffected over the same period. However, increasing the exposure times to 1 year caused gradual disappearance of the outer zinc layer in all cases, leaving a dark-grey surface which tended to powder.

At 250°C (480°F), the initial effect of heating was thermal etching of the surface. Separation of the outer zinc layer was found to occur at an early stage (as detected by applying scotch tape to the coating surface and then pulling it off). This procedure readily removed the zinc from the outer coating of CT after 4 days, and of DT and ET after 1 week. Longer exposure times, up to 8 weeks, increased the ease of removal. More prolonged heating, for from 12 to 52 weeks, again caused gradual and complete disappearance

of the outer layer, exposing the dark zeta-phase surface.

At 300°C (570°F), separation of the outer zinc occurred after 8 hours with CT, and 16 hours with ET and DT. Continued heating for up to 4 weeks reduced the thickness of the zinc layer remaining to a point where rubbing exposed the zeta layer. Longer times produced a light-grey surface on CT which ultimately resulted in a hard, abrasion-resistant finish at about 12 weeks, with little change thereafter to 24 weeks. In contrast, the surfaces on ET and DT retained a powdery chalky grey appearance in the later stages of the 24-week exposure period. For equivalent exposure times, therefore, a more advanced reaction stage was indicated for CT.

In the short-term tests at 400°C (750°F), peeling of the zinc layer on CT occurred within 1/2 hr. Further heating to 16 hours caused gradual thinning of the zinc layer until only small, discontinuous patches remained on the otherwise dark zeta surface exposed. At any intervening stage, the zinc still present could be readily chipped away, or peeled by the tape method described earlier. Beyond 16 hours, transformation to a light-grey finish occurred rapidly and there was little further change to 4 weeks. The surface produced was hard and abrasion-resistant, and showed no tendency to flake or peel.

Stripping Tests and Metallography

(a) Exposure at 200°C (390°F)

Figures 4 to 6 show that the iron content of the outer coatings on the tubing products increased slowly with time at 200°C (390°F). Similar but less consistent trends applied with the inner coatings and in general the iron values were slightly higher, except with DT where the reverse was true. These differences presumably relate to the more pronounced variations in as-galvanized thickness and uniformity of the inner coatings.

Microstructurally, local separation at the zinc-zeta interface on CT occurred as early as 6 weeks at this temperature. More or less complete bond rupture in the outer coating at 16 weeks is shown in Figure 8(a), and local disappearance of zinc is also evident. At 24 weeks, only scattered patches of zinc remained, which, although detached, were apparently keyed in place as described earlier. Of interest in Figure 8(b) is the lesser degree of interface separation with the thicker interior coating. The typical area shown indicates that the irregular, serrated interface was pockmarked with porosity voids but the zinc-zeta bond was otherwise intact. This change in behaviour may have been related to more sustained migration of zinc atoms to the reacting interface because of the thick zinc layer present. Another possibility is that internal compression forces were developed, owing to the volume increase from iron-zinc alloy growth, and tended to hold the zinc layer more firmly in place on the concave inner surface. On the outside, growth of iron-zinc alloy would induce tension forces at the interface, thereby promoting a more rapid detachment of the zinc layer.

Heating of Tubing CT for 1 year produced the structures shown in Figures 8(c) and (d). A dense zeta layer with numerous vertical cracks was the predominant constituent.

The improved resistance to peeling of the seamless tubing (DT) was reflected in the microstructure, and scattered interface voids as in Figure 9(a) represented the extent of bond deterioration after 24 weeks at 200°C (390°F). In this case, both inner and outer coatings which, it will be recalled, were of approximately similar thickness as-galvanized, were affected to about the same degree. Tubing ET, on the other hand, was only slightly better than CT, as may be seen by comparing the outer coating samples in Figures 8(a) and 9(c). In a further similarity to CT, the very thick irregular inner coating on ET after 24 weeks also showed void formation rather than a continuous interface separation. Another microstructural feature of interest with ET was the distinct duplex-etching

structure of the delta-prime phase, as in Figure 9(c). The light and dark regions are consistent with the low- and high-iron constituents of this phase, usually referred to respectively as "palisade" and "coherent" delta.

After 1 year at this temperature, the outer coatings on DT and ET appeared as in Figures 9(b) and (d) respectively. Vertical cracking in the columnar zeta-phase was evident and frequently penetrated into the duplex-etching delta-prime layer. The uniform thickness of the coating as a whole, at this stage, is to be noted.

(b) Exposure at 250°C (480°F)

The iron-content data at 250°C (480°F) more clearly revealed the dependence of iron build-up on the initial coating thickness, and on the thickness of the outer zinc layer. Minimal change with heating time was found with the thinnest coating, namely that on the outside of CT (Figure 4). Significantly higher parabolic trends were indicated for the thicker, outer coatings on DT and ET (Figures 5 and 6). As was to be expected, proportionately still greater increases with time were realized with the heavier interior coatings. In this case, the trends for all three products were approximately similar. To what extent variable steel-base reactivity on the opposite surfaces may also have contributed to the different behaviour of the inner and outer coatings is unknown.

The microstructures for Tubing CT showed that small interface porosity voids were formed in the outer coating within the first day at 250°C (480°F). Separation was almost continuous after 2 days (Figure 10(a)), and only detached patches of zinc remained after one week. The same sequence occurred with the inner coating at a slightly slower rate but, even in this case, complete separation of the zinc layer was apparent after only 4 days. The notably different bond-deterioration behaviour on the inner and outer coatings at 200°C (390°F) was thus much less marked at 250°C (480°F).

From the series of outer coatings shown in Figure 10, it is apparent that in early stages of heating, growth of the zeta and delta-prime phases was combined with dissolution of the detached zinc layer and of the gamma phase layer. This was followed later by thinning of the zeta phase as it was slowly transformed to delta-prime. The complex, irregular growth of the latter, and the reappearance and growth of the gamma phase, are also to be noted. The contrast in outer and inner coating thicknesses after 1 year's heating, which reflect the original as-galvanized thickness variation on Tubing CT, can be seen in Figures 10(d) and (e).

At this temperature, the metallographic evidence of interface separation indicated that DT and ET were only moderately better than CT. In each case, 1 week's exposure was sufficient to produce more or less complete detachment of the zinc layer from the outer coating. On the inside, large voids formed in 2 weeks as in Figure 11(a), although the interface bond between them frequently remained intact. It must be noted that the large size of the voids was, in part, probably related to tearing out, during polishing, of zeta crystals undermined by reaction depletion of the surrounding zinc matrix. Within 4 weeks, no zinc was evident on any samples except in detached patches on the heavy interior coating of ET.

Much longer exposures produced typical structures on DT as in Figures 11(b) and (c), and in Figure 12 for ET. These were again highlighted by a columnar zeta-phase structure, and the characteristic duplex-etching intermixture of constituents forming the delta-prime phase layer. Another observation with both products was that the gamma-phase originally present disappeared in early stages of heating, to reappear again later as a uniform continuous layer next to the steel base. Its thickness was variable on the different products, and on inner and outer surfaces of the same product.

(c) Exposure at 300°C (570°F)

The curves in Figures 4, 5 and 6 reflect the still greater iron-zinc alloying rate at 300°C (570°F), most particularly in the early stages of exposure. Maximum iron build-up with time was associated with the thick interior coatings, and only with the seamless tubing (DT) was there a close similarity in behaviour between the inner and outer coatings. This response, and the respectively larger differences evident for CT and ET in Figures 4 and 6, were, as discussed earlier, apparently related to the original coating thickness and/or to the amount of zinc available for reaction from the outer layer. The latter was indicated to be a dominant factor, even though the layer was effectively detached at a very early stage.

The microstructural effects at this temperature essentially reproduced those found at the lower temperatures with, of course, more rapid onset of the various deterioration stages and more advanced long-term transformation changes. For example, the coatings on CT and ET revealed evidence of zinc separation within 4 hours. Tubing DT retained only a slight advantage at this temperature, since the same stage was reached in 8 hours. With all three products, most of the detached outer layer disappeared in less than 1 week, except in the thicker areas. Typical reaction effects with more prolonged heating of CT are shown in Figure 13. The characteristic transformation of the zeta phase to delta-prime in 4 weeks, leading to a heavily fissured outer band in the latter, can be seen in Figure 13(b). The depth of fissuring appeared to coincide with the boundary of the high-iron coherent-delta constituent. At 24 weeks, a complex intermixture of delta-prime and an unidentified dark-etching material, presumably an oxidation product, formed the bulk of the coating, as in Figure 13(d).

Reference was made previously to the hard, abrasion-resistant finish developed on the exterior of CT after 12 weeks at 300°C (570°F). Earlier occurrence of the hard delta-prime phase at the surface, due to

the shorter diffusion path through the thin coating present, was the probable explanation. Irregular fissuring of this layer, as evident in Figure 13, may also have been involved. In contrast, both DT and ET developed a fine filigree break-up (Figure 14), apparently as a result of transformation from the distinctive columnar zeta-phase structure evident with these products.

For all exposure times tried at 300°C (570°F), no evidence was found of intergranular penetration into the steel base.

(d) Exposure at 400°C (750°F)

The highly accelerated reaction effects developed in the preliminary heating tests made on Tubing CT at 400°C (750°F) are illustrated in Figure 15. Separation of the zinc layer was complete within the first half-hour, and probably in the first few minutes as suggested from other related work on conventional galvanized coatings[5]. Rapid disappearance of the detached zinc was combined with accelerated transformation of the zeta phase, so that at 2 hours the coating consisted almost entirely of the delta-prime layer as in Figure 15(b). The appearance of this phase at the surface coincided with the transition to a light-grey abrasion-resistant finish, described earlier. Subsequent fissuring of the palisade delta, and growth of the gamma layer to a considerable thickness, can be seen in Figures 15(b) and (c).

Although intergranular attack of the steel base was not developed in the characteristic manner in these tests, there was evidence of intermetallic compound formation. A typical distribution of the randomly scattered compound particles growing down into the steel can be seen in Figure 15(d). It was again established from other work that such particles nucleated intergranularly and, depending on the time-temperature conditions of exposure, could link up in a grain-boundary network pattern.

Mechanical Tests

The mechanical properties for samples of Tubing CT in the as-received condition and after heating at 400°C (750°F) are recorded in Table 6. Exposures of up to 2 weeks produced relatively minor changes, including a decrease in ultimate tensile strength and an increase in elongation. The yield strength was not significantly altered. Negligible embrittlement of the steel base was therefore indicated, despite the incidence of intergranular compound formation described in the previous section. In view of this behaviour, tensile tests were not attempted on samples heated at the lower temperatures.

RESULTS FOR ANGLE AND BAR PRODUCTS

Surface Effects

Heating at 200°C (390°F) for up to 24 weeks had little effect on the coating on Angle DA but, in the interval to one year, the outer zinc layer separated and gradually disappeared. The time for separation could not be determined on the single sample given this prolonged treatment. Angle CA and Bar CB were not tested at this temperature.

At 250°C (480°F), the coating behaviour for all three products was similar to that for Tubing DT, starting with thermal etching of the surface at 4 days, followed by lack of adhesion (tape test) of the outer zinc layer after about 1 week. Continued heating resulted in thinning of the zinc, but sufficient remained to permit peeling after 12 weeks with Angle DA, and 20 weeks with Angle CA and Bar CB. At 24 weeks the underlying zeta phase was completely exposed.

The surface deterioration sequence described above was essentially complete in each case in 2 weeks or less at the maximum temperature of 300°C (570°F). At this stage, some patches of zinc remained on only the

most heavily coated Angle CA. With more prolonged heating (up to 24 weeks), a chalky grey, powdery surface was uniformly developed on each material. This could be readily removed by scratching.

Stripping Tests and Metallography

(a) Exposure at 200°C (390°F)

Figure 7 shows the negligible change in iron content of the coating on Angle DA after 24 weeks at 200°C (390°F). Apart from some angular, facetted pitting at the zinc surface, the coating microstructure was not significantly altered from the as-received condition illustrated in Figure 3(a). In the further interval to one year, most of the separated zinc layer had disappeared and irregularities in thickness of the iron-zinc alloy layers were evened out, producing uniformly developed layers of the three phases, as in Figure 16(a). The duplex-etching delta-prime layer was the predominant constituent. The similarity to structures found on Tubings DT and ET (Figures 9(b) and (d) respectively), which were given the same treatment, is to be noted.

(b) Exposure at 250°C (480°F)

At 250°C (480°F), the iron content curves for Angle DA and Bar CB in Figure 7 define a moderate parabolic change not unlike that found with the tubing materials. It is of interest that the trends for these two materials were similar even though the angle was a rimming steel and the bar was semi-killed. The expected variation in the reaction rate because of steel-base composition and microstructure (Figure 1) was thus not realized. A representative coating microstructure after 24-week heating is shown in Figure 16(b), and illustrates the uniform layered structure developed, which was composed mainly of the zeta phase. Somewhat more typical of a semi-killed steel was the much higher reactivity of Angle CA at this temperature (Figure 7). The response in this case was to some extent predictable, since the as-galvanized coating microstructure

in Figure 3(b) was indicative of a reactive steel. The evident irregularity in reactivity at different points on the steel surface was retained throughout the different heating periods. As a result, the transformed coating developed an appearance as in Figure 17(a), with very thick fissured outbursts of the delta-prime phase being separated by areas showing more normal iron-zinc alloy growth.

(c) Exposure at 300°C (570°F)

At 300°C (570°F), Figure 7 indicates that the iron increase with time reached gross proportions with Angle DA, and still more so with Angle CA. The reaction rate on Bar CB was significantly lower and corresponded to the behaviour of the thicker coatings on the tubing products. The widely different response of these two semi-killed products (CA and CB), apparent at 250°C (480°F), was thus confirmed. This suggests that the major dependence of steel-base reactivity on the silicon content (up to 0.10%), as claimed by Sandelin[13], is not all inclusive, and that other surface factors connected with steel-base processing and history must also exert some effect. Equally anomalous was the high reactivity of the rimming-grade Angle DA. The moderately high phosphorus content, combined with low silicon, in this case may have been responsible. However, other, unknown factors must again have been involved, since this effect was observed only at 300°C (570°F) and not at the lower test temperatures.

The microstructures in this series revealed that separation and disappearance of most of the outer zinc layer, and the subsequent transformation and fissuring of the iron-zinc alloy layers, were largely complete within 1 to 2 weeks. At this and longer exposures, the typical appearance of the coatings varied between those shown in Figures 16(c) and 17(b), for Angles DA and CA respectively. Differences in thickness, uniformity and iron-zinc alloy constituent structure were evident but,

in general, the coating deterioration features on all three products largely reproduced those observed at 250°C (480°F).

The only significant effect not previously observed in any test at and below 300°C (570°F), was a tendency to intergranular penetration of the steel base with Angle DA. This was initially developed at 2 weeks and extended several grain-layers deep into the steel at 24 weeks as shown in Figure 16(c). Deepest penetration took the form of beads of grain-boundary intermetallic particles of the type found with Tubing CT heated at 400°C (750°F). From this and other evidence in earlier work on continuous strip[1][2], it thus appears that rimming-grade steel is more prone to intergranular attack by zinc. To what extent this may be related to reaction with cementite distribution at the ferrite grain boundaries is unknown.

Bend Tests

Although the depth of intergranular penetration of Angle DA in the above tests was minor in comparison with the section thickness, it was considered desirable to examine this further by bend tests. One-inch-wide pieces were removed from the legs of various samples and subjected to a zero-radius 180° bend by pressing between the platens of a tensile machine. Bending was first initiated by pressing a 3/4-in.-diameter (2-cm) mandrel down on the test pieces, which were roll-supported mid-way between the centre and ends of the 7-in. (17.5-cm) lengths used. Metallographic effects observed on the exterior bend of typical samples, inclusive of one heated at 400°C (750°F), are reproduced in Figure 18.

It can be seen that, with increasing exposure temperature, vertical cracking of the coating was more localized. Larger and larger blocks of iron-zinc alloy remained intact, thereby reducing the area of the steel surface which was subject to deformation and yielding in the bending process. This presumably accounts in part for the gross

"necking" gaps formed at the maximum temperature of 400°C (750°F). Yielding was initiated at preformed intergranular cracks and, to this extent, the penetration into the steel base during heating was detrimental. Nevertheless, the "rounded" form of the gaps suggests significant ductility below the crack roots. Embrittlement as such was thus apparently minimal for the type of stressing involved in the slow-bend test. It will be appreciated that a similar response cannot be extrapolated to notch-toughness impact tests, and more so because carbon rimming steels have inherently poor notch-toughness characteristics in any case.

SUMMARY AND DISCUSSION

This investigation has confirmed that heating of conventional galvanized coatings in an air environment will induce separation of the outer zinc layer at a temperature as low as 200°C (390°F), if the heating time is sufficiently prolonged. Continuous exposure up to several months can be tolerated without such failure, depending on the microstructural characteristics of the coating. At higher temperatures the process is considerably accelerated; at 300°C (570°F), for example, it is well advanced in a few hours.

Study of the mechanism of separation was beyond the scope of the investigation but it was apparent that it involved reaction dissolution of the zinc matrix in the interstices of the bordering fringe of zeta-phase crystals. The gap so formed widened with time along the entire interface as more zinc was consumed to form iron-zinc alloy. No evidence was found to suggest that the difference in coefficient of expansion of zinc and iron contributed to destruction of the zinc-zeta bond. However, specific tests aimed in this direction were not attempted.

In subsequent stages, gradual disappearance of the detached zinc layer occurred as long as it remained in place next to the zeta layer. This effect was observed with all products tested. It was not possible to devote attention to examination of the process by which the detached layer was used up. Presumably oxidation, and probably volatilization to some extent, were contributory factors, but various observations suggested that continued transport and reaction of zinc across the separation gap may also have been involved.

In combination with dissolution of the zinc layer, diffusion transformations within the iron-zinc alloy layers produced varying amounts of the different phases, depending on the time-temperature conditions. Growth of the zeta phase predominated at first, but this layer eventually disappeared, being replaced by increasing proportions of the higher-iron delta-prime and gamma phases. The exposed delta-prime was, in turn, heavily fissured, due to continued inward diffusion of zinc and/or oxidation effects. However, under all conditions tried, one or more of the alloy layers remained adherent to the steel base. There was no tendency for the layers to spall off, and the cathodic and barrier protection characteristics of the coating were thus retained.

The onset of intergranular penetration of the steel base was indicated to be principally temperature-dependent and restricted to an undefined level above 300°C (570°F). An exception to this was the behaviour of a rimming-grade steel (Angle DA) which showed well-defined grain-boundary attack at this temperature. The degree of penetration was minor in comparison with the total section thickness, and embrittlement therefrom was indicated to be negligible in so far as slow-bending type of deformation was concerned. With such stressing, coating ductility was expectedly poor under all conditions, although the tendency of the coating to crack and spall was variable and dependent on the temperature of heating.

From the results it was apparent that the various products tested exhibited significant differences with respect to peeling and subsequent deterioration of the coatings. One factor or a combination of several factors was responsible. These included the total coating thickness, the relative thicknesses of outer zinc and iron-zinc alloy, the uniformity of the individual layers, the geometry of the coated surface, and the inherent chemical reactivity of the steel base as related to its composition, structure, smoothness and processing history.

Considering the tubing products, the influence of the coating microstructural factors was most prominently reflected in the better resistance to peeling of Tubing DT, particularly at 200°C (390°F). Improved uniformity in the iron-zinc alloy coating remaining after long-term exposure was also apparent. The response of this product was associated with its superior as-galvanized coating uniformity (both inside and outside), which was highlighted by more evenly developed iron-zinc alloy layers, and an equivalent thickness of outer zinc also showing good uniformity. These characteristics were apparently related to the cold-drawn nature of the steel surface and to the galvanizing processing.

Further defining the relationship between the peeling tendency and the coating microstructure was the rapid onset of peeling of the thin outer coatings on Tubings CT and ET. As an opposite extreme was the behaviour of the thick interior coatings on these products which, it will be recalled, were composed mainly of an excessively heavy, non-uniform zinc layer. Although this type of coating, in combination with an apparent surface-geometry effect, appeared to confer good resistance to peeling, a deposit of this kind would not, for various other reasons, be considered desirable.

From a practical point of view, the behaviour of the tubing products tested suggests that approximately equivalent thicknesses of iron-zinc alloy and outer zinc, totalling between 1.75 and 2.25 oz/sq ft

(535 and 685 g/m^2), represent a near-optimum microstructure. This should provide the best resistance to peeling deterioration, as well as improved long-term cathodic and barrier protection, in an elevated-temperature air environment around 200°C (390°F). To what extent conventional galvanizing production of such a desirable coating can be achieved would appear to be dependent on the nature and chemical reactivity of the steel-base surface, as well as on the care and control exercised in galvanizing processing.

With respect to the thick-wall angle and bar products, the good resistance to peeling by Angle DA at 200°C (390°F) corresponded to that of Tubing DT. The desirability of uniformly distributed and near-equal thicknesses of iron-zinc alloy and outer zinc thus appeared to be confirmed. Although not tested at this temperature, equally good behaviour could probably be expected with the semi-killed Bar CB, because of its indicated low iron-zinc alloying reactivity at higher temperatures. It will be noted that the as-galvanized coating thickness on this product and Angle DA was near the high end of the range recommended above. Less satisfactory response at 200°C (390°F) could be assumed for the much thicker coating on the high-reactivity Angle CA. This follows from the highly irregular, fissured coating-structure found at the higher test-temperatures tried.

The anomalous high-temperature deterioration characteristics of the semi-killed products (Angle CA and Bar CB) emphasize the inherent product variability which can apparently occur with such classes of material. This could not be related to steel-base composition and microstructure, which were identical for both products, and it must be presumed that other, unknown factors connected with steel processing and fabrication history were responsible. Further evidence of the same effect was provided by the high reactivity of the rimming-grade steel (Angle DA) at 300°C (570°F), and by its unique tendency to intergranular penetration. As noted, the degree of such attack was found to be non-embrittling in so far as slow-bending deformation was concerned.

CONCLUSIONS

In an air environment, conventional galvanized coatings may withstand long-term continuous exposure of up to several months at 200°C (390°F) without separation of the outer zinc layer. The incidence of such failure will depend on the microstructural characteristics of the coating. Higher temperatures progressively accelerate the separation process to the point where it requires only a few hours at 300°C (570°F).

Secondary deterioration involves gradual disappearance of the detached zinc layer, in combination with diffusion-controlled transformation changes in the underlying iron-zinc alloy layers. In advanced stages, the coating remaining consists of the delta-prime and gamma iron-zinc phases, and severe fissuring of the former is evident. Intergranular penetration of the steel base can also occur.

Apart from the predominant effect of the time-temperature conditions, the rate of the deterioration process is influenced by coating thickness, the relative thicknesses of outer zinc and iron-zinc alloy, and by the uniformity of the individual layers. An additional important factor is the inherent chemical reactivity of the steel base as determined by its composition, microstructure, smoothness, and processing history. By its effect on the length of the diffusion path, or the rate of the iron-zinc diffusion reactions, any of the factors named can apparently affect the speed and degree of coating deterioration for a given set of heating conditions.

At the industry-recommended limiting service temperature of 200°C (390°F), superior resistance to zinc-layer peeling was indicated for one of the tubing and one of the angle products (DT and DA, respectively). Better long-term cathodic and barrier protection was also suggested in these cases, because of improved uniformity and continuity in the iron-zinc-alloy layer structure developed on prolonged heating at this temperature.

This behaviour appeared to be related to more-nearly-optimum coating characteristics, i.e. uniformly distributed and approximately equivalent thicknesses of iron-zinc alloy and outer zinc layer, totalling between 1.75 and 2.25 oz/sq ft (535 and 685 g/m^2). Steel-base factors which influenced the diffusion-reaction activity during heating also apparently contributed to this improved performance.

In all tests at 200°C (390°F), the iron-zinc-alloying reaction rate (based on the iron content of the coatings) was observed to increase slowly with time. However, for one or more reasons connected with the factors mentioned above, the other products tried were suggested to be less satisfactory than Tubing DT and Angle DA.

At higher temperatures, the resistance to peeling was poor in all cases. However, the structural and protective qualities of the coatings remaining on the different products after extended exposure at 250°C (480°F) appeared similar to those at 200°C (390°F). Thus, assuming that peeling of the zinc layer could be ignored in a service application, useful long-term protection could probably be obtained at temperatures as high as 250°C (480°F). To what extent this would actually be achieved at this or lower temperature levels would, of course, be dependent on the nature and severity of the corrosion environment in the particular application. Tests in this direction were beyond the scope of this investigation.

REFERENCES

1. J. J. Sebisty, R. H. Palmer and D. F. Watt - "The Elevated-Temperature Behaviour of Continuous-Strip Galvanized Coatings" - Physical Metallurgy Division Internal Report PM-R-63-13, Mines Branch, Department of Energy, Mines and Resources, Ottawa (1966).

2. J. J. Sebisty - "Continuous-Strip Galvanized Coatings at Elevated Temperatures" - Electrochemical Technology 6(5), 330-336 (1968).

3. A. A. Hershman and N. D. Neemuchwala - "The Peeling of the Zinc Layer in Galvanized Coatings" - British Corrosion Journal 1 (2), 51-52 (1965).

4. J. J. Sebisty and D. Papenfuss - Discussion of paper "The Peeling of the Zinc Layer in Galvanized Coatings" - ibid. 1 (5), 251 (1966).

5. J. J. Sebisty and D. Papenfuss - unpublished data (1966).

6. K. Oganowski - "A Look at Coatings on Steel" - Sheet Metal Industries 41 (9), 675-686 (1964).

7. Joint Discussion, Proc. of Second International Galvanizing Conference, Zinc Development Assoc., London, 40 (1952).

8. Joint Discussion, Proc. of Third International Galvanizing Conference, Zinc Development Assoc., London, 56-57 (1954).

9. Joint Discussion, Proc. of Sixth International Galvanizing Conference, Zinc Development Assoc., London, 95 (1961).

10. H. Bablik, F. Gotzl and E. Nell - "The Cooling of Galvanized Products" - Metalloberflache 9 (8), 643-645 (1955).

11. J. Teindl and O. Blahoz - "Causes of Peeling of Zinc from Galvanized Steel Sheet" - Hutnicke Listy 21 (3), 179-181 (1966).

12. J. J. Sebisty - "Metallurgical Examination of Galvanized Tubing" - Mines Branch Report IR 66-4, Department of Energy, Mines and Resources, Ottawa (1966).

13. R. W. Sandelin - "Modern Trends in Steel as Affecting Hot Dip Galvanizing" - American Hot-Dip Galvanizers Association Annual Meeting (Arizona), April 1963.

14. D. H. Rowland - "Metallography of Hot-Dip Galvanized Coatings" - Trans. American Society for Metals 40, 983-1011 (1948).

- - - - -

JJS:RHP:(PES):KW

TABLE 1

Pickling Data

Product	Solution	Temperature (°C)	Temperature (°F)	Time (min)	Rinse
Tubing					
CT	H_2SO_4 (90 g/l)	75	165	15	Yes
DT	HCl (110 g/l)	30	85	50	No
ET	H_2SO_4 (120 g/l)	80	175	45	Yes
Angle					
DA	HCl (110 g/l)	30	85	50	No
CA	H_2SO_4 (60g/l)	55	120	47	Yes
Bar					
CB	H_2SO_4 (60 g/l)	55	120	47	Yes

TABLE 2

Galvanizing Data

Product	Fluxing Method	Bath					Immersion Time (min)	Withdrawal Speed		Post Treatment
		Composition (%)			Temperature					
		Fe	Pb	Sn	(°C)	(°F)		ft/min	cm/sec	
Tubing										
CT	Dry	*	*	*	455	850	*	*	*	*
DT	Wet	0.035	1.46	0.056	460	860	5.5	1.7	0.9	Air-cool
ET	Dry and Wet	0.048	1.20	0.006	455	850	3.0	1.7	0.9	Water-quench
Angle										
DA	Wet	0.035	1.46	0.056	460	860	8.0	1.7	0.9	Air-cool
CA	Dry and Wet	0.033	1.20	**	455	850	4.5 to 7.0	7.0	3.5	***
Bar										
CB	Dry and Wet	0.033	1.20	**	455	850	4.0 to 6.0	8.0	4.0	***

* Bath sample and other data not provided.

** Not detected.

*** Air-cooled for 2 min and water-quenched at 70°C (160°F).

TABLE 3

Chemical Composition of Steel Base

Product	Steel Composition (%)									
	C	P	Mn	S	Si	Al	Cu	Ni	Cr	N
Tubing*										
CT (welded)	0.10	0.002	0.51	0.025	<0.01	<0.01	0.04	0.02	0.07	-
DT (seamless)	0.10	0.007	0.46	0.021	0.01	<0.01	0.19	0.11	0.15	0.007
ET (welded)	0.05	0.044	0.35	0.035	<0.01	<0.01	0.01	0.03	0.03	0.007
Angle**										
DA	0.16	0.032	0.42	0.050	<0.01	n.d.	0.13	0.03	0.07	0.005
CA	0.26	0.003	0.47	0.024	0.07	<0.005	0.04	0.04	0.04	0.003
Bar***										
CB	0.24	0.003	0.50	0.035	0.06	<0.005	0.05	n.d.	0.04	0.002

* 3/4-in. (1.9-cm) standard-weight tubing with 0.113-in. (0.287-cm) wall thickness. Relevant specifications B.S. 1387 and DIN 2391.

** 1-9/16 x 1-9/16 x 1/8 in. (4.0 x 4.0 x 0.3 cm).

*** 2-1/2 x 3/16 in. (6.4 x 0.5 cm).

TABLE 4

Chemical Composition of Coating

Product	Coating Composition (%)					
	Fe	Pb	Sn	Cu	Cd	Sb
Tubing						
CT	4.1	0.61	*	0.02	*	*
DT	4.0	0.63	0.03	*	*	*
ET	3.2	0.64	*	*	*	*
Angle						
DA	4.2	0.55	0.03	*	*	*
CA	3.7	0.75	*	0.02	*	*
Bar						
CB	3.8	0.78	*	0.02	*	*

* Not detected.

TABLE 5

Experimental Program

Product	Exposure		
	Temperature		Time
	(°C)	(°F)	
Tubing			
CT, DT and ET	200	390	2, 4, 6, 8, 12, 16, 20, 24 and 52 wk.
Angle			
DA	200	390	2, 4, 6, 8, 12, 16, 20, 24 and 52 wk.
Tubing			
CT*, DT and ET	250	480	1, 2 and 4 days; 1, 2, 4, 6, 8, 12, 16, 20 and 24 wk.
Angle			
DA and CA	250	480	1, 2 and 4 days; 1, 2, 4, 6, 8, 12, 16, 20 and 24 wk.
Bar			
CB	250	480	1, 2 and 4 days; 1, 2, 4, 6, 8, 12, 16, 20 and 24 wk.
Tubing			
CT, DT and ET	300	570	4, 8 and 16 hr; 1, 2 and 4 days; 1, 2, 4, 6, 8, 12, 16, 20 and 24 wk.
Angle DA and Bar CB	300	570	4, 8 and 16 hr; 1, 2 and 4 days; 1, 2, 4, 6, 8, 12, 16, 20 and 24 wk.
Angle CA	300	570	4, 8 and 16 hr; 1, 2 and 4 days; 1, 2, 4, 6, 8, and 12 wk.
Tubing			
CT	400	750	½, 1, 2, 4, 8 and 16 hr. 1, 2, 7, 14 and 28 days.

*One sample exposed at 250°C (480°F) for 52 wk.

TABLE 6

Mechanical Properties of Tubing CT After 400°C (750°F) Heating Tests

Product	Exposure Time (days)	UTS (kpsi)			YS (kpsi)			El. (% in 2 in.)		
		Av	High	Low	Av	High	Low	Av	High	Low
Tubing										
CT	0	54.2	55.7	53.3	39.4	40.9	37.7	27.9	29.0	27.5
	1	52.3	53.0	51.8	40.0	41.2	38.4	32.0	33.5	31.5
	7	51.4	51.6	51.2	39.9	42.1	38.3	33.4	34.0	32.5
	14	50.4	50.8	49.8	39.0	40.6	37.1	30.1	32.5	28.5

TABLE 7

Stripping-Test Results for Tubing CT*

Product	Exposure					Coating Wt				Iron Content			
	Temperature		Time			Outside		Inside		Outside		Inside	
	(°C)	(°F)	(hr)	(day)	(wk)	(oz/sq ft)	(g/m^2)	(oz/sq ft)	(g/m^2)	(g/m^2)	(%)	(g/m^2)	(%)
Tubing CT	200	390			0	1.04	317	1.88	574	17.2	5.4	19.4	3.4
					2	1.01	308	2.07	632	17.9	5.7	20.1	3.2
					4	0.99	302	2.42	739	17.5	5.8	20.4	2.8
					6	1.02	311	2.14	653	18.0	5.8	20.9	3.2
					8	1.01	308	2.08	635	17.9	5.8	20.6	3.2
					12	1.01	308	2.00	610	18.3	5.9	22.0	3.6
					16	1.01	308	1.84	561	19.0	6.2	25.4	4.5
					20	1.02	311	1.79	546	19.6	6.3	27.9	5.1
					24	1.08	329	2.22	677	20.9	6.3	33.2	5.1
					52	1.11	339	2.35	717	24.2	7.1	42.1	5.9
"	250	480		1		1.20	366	2.68	818	19.7	5.4	22.1	2.8
				2		1.16	354	2.30	702	19.8	5.6	23.6	3.4
				4		0.96	293	2.57	784	20.9	7.1	25.3	3.2
					1	1.10	335	1.82	555	23.8	7.1	31.5	5.7
					2	0.98	299	2.52	769	23.4	7.8	41.7	5.4
					4	1.12	342	1.80	549	25.1	7.4	34.9	6.4
					6	1.18	360	2.10	641	28.3	7.8	40.0	6.4
					8	0.98	299	2.23	681	25.7	8.6	49.7	7.3
					12	1.02	311	2.28	696	26.8	8.7	52.2	7.5
					16	0.98	299	2.37	723	27.0	9.0	55.7	7.7
					20	0.98	299	2.29	699	27.3	9.1	55.2	7.9
					24	1.00	305	2.28	696	27.8	9.2	57.5	8.3
					52	1.01	308	2.32	708	32.0	10.4	63.0	8.9
"	300	570	4			1.23	375	2.66	812	22.6	5.9	24.3	3.0
			8			1.09	332	3.21	980	22.0	6.6	25.6	2.6
			16			1.08	329	1.88	574	24.2	7.3	28.2	4.9
				1		1.17	357	2.76	842	30.0	8.4	40.3	4.8
				2		1.18	360	2.70	824	29.1	8.1	41.1	5.0
				4		1.20	366	2.64	806	31.9	8.7	45.8	5.7
					1	1.09	332	2.07	632	31.4	9.4	40.2	6.4
					2	1.26	384	2.60	794	39.0	10.1	56.4	7.1
					4	1.24	378	2.14	653	45.2	11.9	62.0	9.5
					6	1.22	372	2.06	629	47.3	12.7	63.3	10.1
					8	1.32	403	2.33	711	47.1	11.6	68.9	9.7
					12	1.33	406	2.71	827	46.7	11.5	72.5	8.8
					16	1.34	409	2.38	726	50.4	12.3	77.7	11.0
					20	1.31	400	2.37	723	47.0	11.7	79.6	11.0
					24	1.33	406	2.46	751	51.6	12.7	83.8	11.2

*Average of duplicate determinations.

TABLE 8

Stripping-Test Results for Tubing DT*

Product	Exposure					Coating Wt				Iron Content			
	Temperature		Time			Outside		Inside		Outside		Inside	
	(°C)	(°F)	(hr)	(day)	(wk)	(oz/sq ft)	(g/m^2)	(oz/sq ft)	(g/m^2)	(g/m^2)	(%)	(g/m^2)	(%)
Tubing DT	200	390			0	1.72	525	2.31	706	23.5	4.5	25.6	3.7
					2	1.62	495	2.38	727	22.8	4.6	27.0	3.7
					4	1.83	559	2.85	870	23.4	4.2	27.5	3.2
					6	1.59	486	2.99	913	27.4	5.6	33.3	3.6
					8	1.80	550	1.96	599	26.8	4.9	26.5	4.4
					12	1.67	510	1.54	470	26.8	5.2	22.3	4.7
					16	1.67	510	1.44	440	26.7	5.2	23.1	5.2
					20	1.67	510	1.48	452	27.3	5.3	23.6	5.2
					24	1.66	507	2.20	672	28.7	5.6	28.0	4.2
					52	1.67	510	2.29	699	35.4	7.0	35.1	5.0
"	250	480		1		1.86	568	1.99	608	23.9	4.2	24.1	4.0
				2		1.92	586	2.05	626	23.9	4.1	24.6	3.9
				4		1.83	559	2.05	626	25.2	4.5	24.5	3.9
					1	1.64	501	2.09	638	29.8	6.0	27.1	4.3
					2	1.78	544	2.47	754	31.5	5.8	30.6	4.1
					4	1.71	522	2.53	772	34.9	6.7	37.5	4.8
					8	1.69	516	2.75	840	37.6	7.2	43.2	5.1
					12	1.62	495	2.96	904	39.4	8.0	53.9	6.0
					16	1.70	519	2.47	754	43.2	8.3	53.3	7.0
					20	1.73	528	2.20	672	45.4	8.6	46.7	7.3
					24	1.71	522	2.01	614	45.0	8.6	46.0	7.5
"	300	570	4			1.85	565	2.64	806	26.0	4.6	28.2	3.5
			8			1.86	568	2.62	800	29.6	5.2	30.9	3.9
			16			1.95	596	2.68	818	34.4	5.8	35.6	4.3
				1		1.84	562	2.11	644	36.9	6.6	36.9	5.7
				2		1.76	538	2.07	632	44.5	8.3	46.6	7.4
				4		1.78	544	2.21	675	45.4	8.3	47.5	7.0
					1	1.90	580	2.76	843	47.0	8.1	56.5	6.7
					2	1.98	605	2.75	840	48.5	8.0	62.9	7.5
					4	2.02	617	2.71	828	64.0	10.4	63.9	9.6
					6	1.85	565	2.61	797	62.6	11.1	74.4	9.3
					8	1.98	605	2.67	815	73.2	12.1	83.5	10.5
					12	1.83	558	2.37	723	70.8	12.6	77.9	10.8
					16	1.94	592	2.57	784	75.6	12.7	81.3	10.3
					20	1.88	574	2.53	773	73.3	12.8	83.8	10.8
					24	1.83	559	2.41	736	72.2	13.0	80.5	10.9

*Average of duplicate determinations.

TABLE 9

Stripping-Test Results for Tubing ET*

Product	Exposure					Coating Wt				Iron Content			
	Temperature		Time			Outside		Inside		Outside		Inside	
	(°C)	(°F)	(hr)	(day)	(wk)	(oz/sq ft)	(g/m^2)	(oz/sq ft)	(g/m^2)	(g/m^2)	(%)	(g/m^2)	(%)
Tubing ET	200	390			0	1.51	461	2.96	904	20.2	4.4	23.1	2.6
					4	1.54	470	2.91	889	21.8	4.6	20.0	2.3
					8	1.61	492	3.58	1093	21.9	4.4	24.2	2.2
					12	1.59	486	3.56	1087	23.5	4.9	26.5	2.4
					16	1.60	489	3.64	1112	22.4	4.6	25.8	2.3
					20	1.61	492	3.50	1069	23.8	4.8	25.5	2.4
					24	1.59	486	3.50	1069	25.3	5.2	27.0	2.5
					52	1.54	470	3.05	932	32.0	6.8	36.0	3.9
"	250	480		1		1.49	455	2.97	907	20.9	4.6	26.3	2.9
				2		1.57	480	3.59	1096	22.6	4.7	24.9	2.3
				4		1.57	480	3.36	1026	25.0	5.2	25.7	2.5
					1	1.47	449	2.94	898	23.5	5.1	29.0	3.2
					2	1.65	504	3.47	1060	31.6	6.3	34.8	3.3
					4	1.63	498	3.45	1054	35.3	7.1	40.3	3.8
					6	1.62	498	3.50	1069	33.5	6.8	41.4	3.9
					8	1.61	492	3.55	1084	35.6	7.2	41.6	3.8
					12	1.64	501	3.27	999	39.9	8.0	51.2	5.1
					16	1.63	498	3.59	1096	39.3	7.8	56.8	5.2
					20	1.62	495	2.78	849	40.1	8.1	57.8	6.8
					24	1.60	489	3.42	1045	40.7	8.3	58.1	5.6
"	300	570	4			1.40	427	2.54	775	21.4	5.0	24.2	3.1
			8			1.44	440	2.77	846	21.9	5.0	25.8	3.1
			16			1.41	431	2.92	892	24.2	5.6	29.4	3.2
				1		1.44	440	2.95	900	27.4	6.2	33.4	3.7
				2		1.44	440	3.34	1020	29.7	6.7	35.6	3.5
				4		1.43	431	3.36	1026	33.2	7.6	40.9	3.7
					1	1.48	452	3.75	1145	37.4	8.2	49.7	4.3
					2	1.55	473	3.75	1145	43.2	9.2	60.7	5.3
					4	1.48	452	2.94	898	41.5	9.1	63.9	7.4
					6	1.66	507	3.60	1099	48.2	9.5	65.3	5.9
					8	1.75	535	3.76	1148	55.7	10.5	75.8	6.6
					12	1.69	516	3.55	1084	56.5	10.9	77.0	7.1
					16	1.60	488	2.54	775	56.0	11.4	82.4	10.6
					20	1.61	492	3.01	919	56.6	11.5	78.2	8.5
					24	1.66	507	3.19	974	65.5	12.9	83.7	8.6

*Average of duplicate determinations.

TABLE 10

Stripping-Test Results for Angle CA*

Product	Exposure					Coating Wt		Iron Content	
	Temperature		Time						
	(°C)	(°F)	(hr)	(day)	(wk)	(oz/sq ft)	(g/m^2)	(g/m^2)	(%)
Angle CA	250	480		0		3.88	1185	43.0	3.7
				1		4.28	1307	43.0	3.3
				2		4.33	1322	44.4	3.4
				4		4.52	1380	47.8	3.5
					1	4.35	1328	46.4	3.5
					2	4.66	1423	54.0	3.8
					4	4.80	1466	71.0	4.8
					8	4.74	1448	83.3	5.7
					12	4.85	1481	87.9	5.9
					16	4.78	1460	88.1	6.0
					20	4.78	1460	89.5	6.2
					24	4.72	1442	89.5	6.2
"	300	570	4			3.58	1093	40.7	3.7
			8			3.82	1167	44.1	3.8
			16			3.63	1109	46.4	4.2
				1		4.19	1280	53.9	4.2
				2		3.87	1182	57.5	4.9
				4		4.15	1267	70.8	5.6
					1	4.15	1267	78.4	6.2
					2	4.25	1298	88.1	6.8
					4	4.49	1371	94.4	6.9
					6	3.74	1142	97.7	8.5
					8	4.73	1445	117.4	8.1
					12	5.23	1597	123.0	7.7

*Average of duplicate determinations.

TABLE 11

Stripping-Test Results for Angle DA*

Product	Exposure					Coating Wt		Iron Content	
	Temperature		Time						
	(°C)	(°F)	(hr)	(day)	(wk)	(oz/sq ft)	(g/m^2)	(g/m^2)	(%)
Angle DA	200	390			0	2.30	702	29.8	4.2
					2	2.41	736	29.2	4.0
					4	2.46	751	28.7	3.8
					6	2.34	715	28.6	4.0
					8	2.18	666	29.1	4.4
					12	2.24	685	28.9	4.2
					16	2.25	687	30.3	4.4
					20	2.21	675	28.3	4.2
					24	2.12	647	31.7	4.9
					52	2.06	629	41.5	6.5
"	250	480		1		2.21	675	28.8	4.3
				2		2.27	693	28.4	4.1
				4		2.29	699	29.4	4.2
					1	2.28	696	33.1	4.8
					2	2.25	687	33.8	4.9
					4	2.11	644	36.3	5.6
					8	2.11	644	39.4	6.1
					12	2.16	660	44.6	6.7
					16	2.02	617	46.5	7.5
					20	2.21	675	47.7	7.1
					24	1.98	605	46.4	7.7
"	300	570	4			2.41	736	32.4	4.4
			8			2.56	782	33.9	4.3
			16			2.60	794	38.1	4.8
				1		2.55	779	39.9	5.1
				2		2.44	745	46.0	6.2
				4		2.41	736	51.6	7.0
					1	2.42	739	65.5	8.9
					2	2.52	770	70.4	9.1
					4	2.42	739	84.0	11.4
					6	2.64	806	89.5	12.1
					8	2.41	736	99.3	12.2
					12	2.39	729	99.5	13.6
					16	2.58	788	107.1	13.6
					20	2.49	760	107.8	14.2
					24	2.47	754	107.1	14.2

*Average of duplicate determinations.

TABLE 12

Stripping-Test Results for Bar CB*

Product	Exposure					Coating Wt		Iron Content	
	Temperature		Time						
	(°C)	(°F)	(hr)	(day)	(wk)	(oz/sq ft)	(g/m^2)	(g/m^2)	(%)
Bar CB	250	480		0		2.36	721	27.2	3.8
				1		2.19	669	27.2	4.1
				2		2.33	712	28.1	4.0
				4		2.35	718	30.0	4.2
					1	2.38	727	29.7	4.1
					2	2.23	681	28.9	4.2
					4	2.52	770	35.4	4.6
					8	2.38	727	43.1	5.9
					12	2.40	733	46.4	6.3
					16	2.39	730	53.2	7.2
					20	2.35	718	50.4	7.1
					24	2.34	715	51.8	7.3
"	300	570	4			2.35	718	30.1	4.2
			8			2.50	762	34.3	4.5
			16			2.46	751	36.0	4.8
				1		2.52	770	39.7	5.1
				2		2.40	733	42.3	5.8
				4		2.54	776	51.2	6.6
					1	2.42	739	54.8	7.4
					2	2.27	693	57.5	8.3
					4	2.44	745	59.2	7.9
					6	2.35	718	60.9	8.5
					8	2.43	742	72.7	9.8
					12	2.47	754	75.7	10.0
					16	2.43	742	77.4	10.5
					20	2.15	657	68.3	10.4
					24	2.34	715	73.7	10.3

*Average of duplicate determinations.

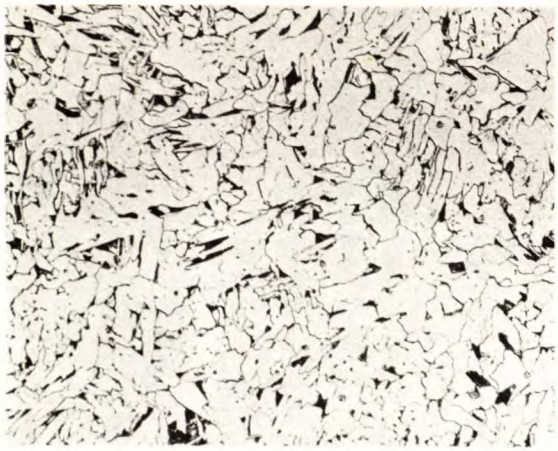

(a) Welded Tubing CT (capped steel)

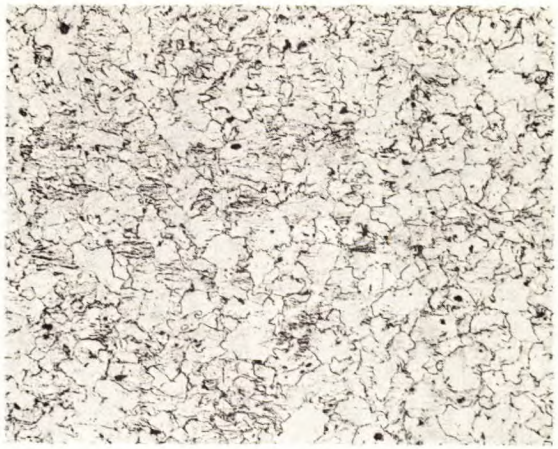

(b) Seamless Tubing DT (rimmed steel)

(c) Welded Tubing ET (rimmed steel)

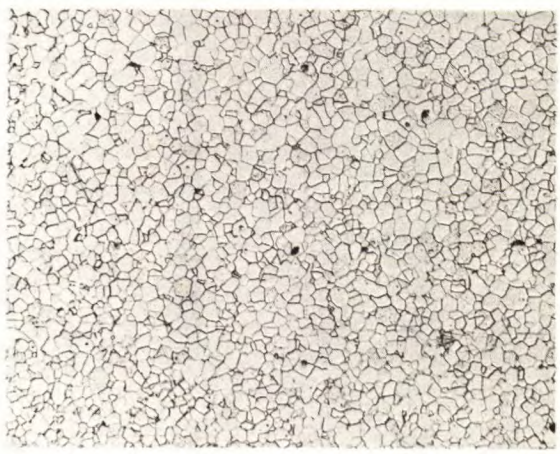

(d) Angle DA (rimmed steel)

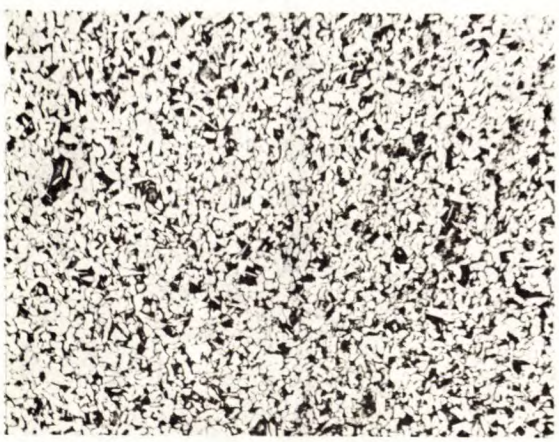

(e) Angle CA (semi-killed steel)

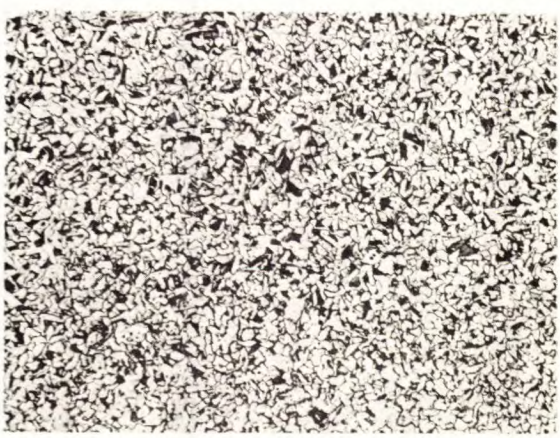

(f) Bar CB (semi-killed steel)

Figure 1. Microstructures of steel base in tubing, angle and bar products. X100.

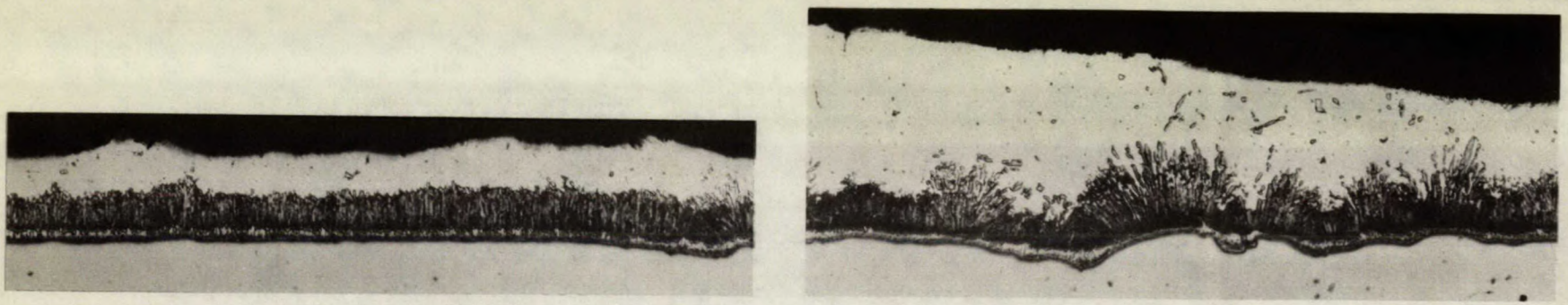

(a) Tubing CT

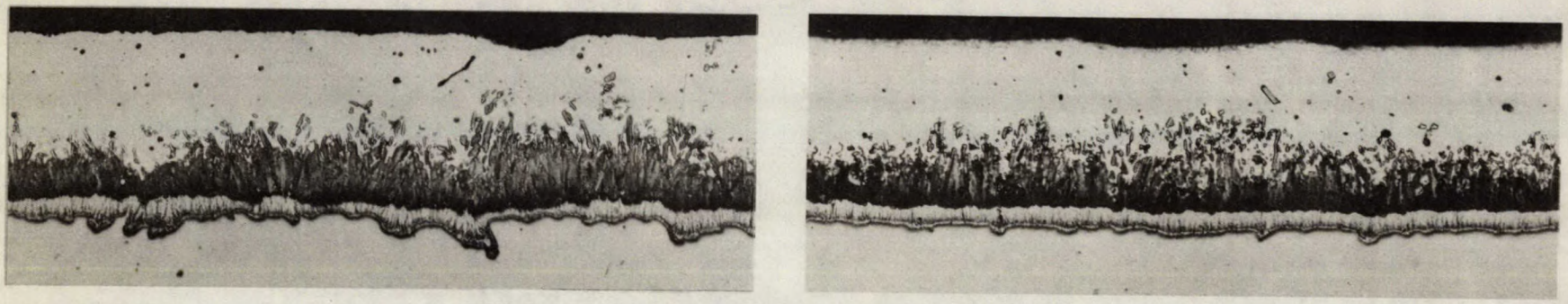

(b) Tubing DT

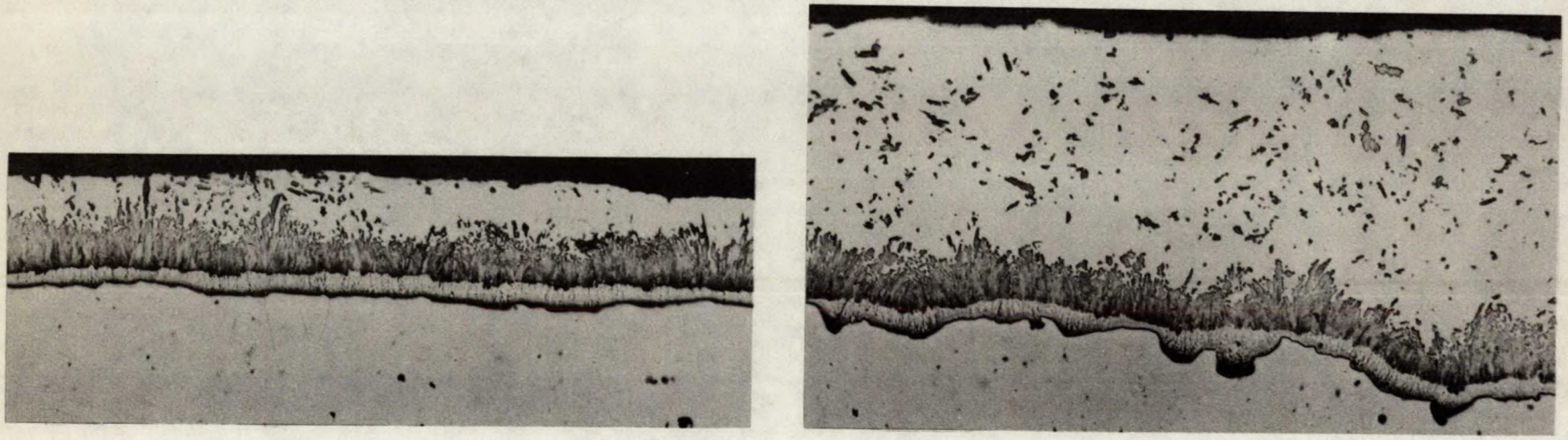

(c) Tubing ET

Figure 2. As-galvanized coatings on tubing products. Outer coatings are on left and inner coatings on right. X250 .

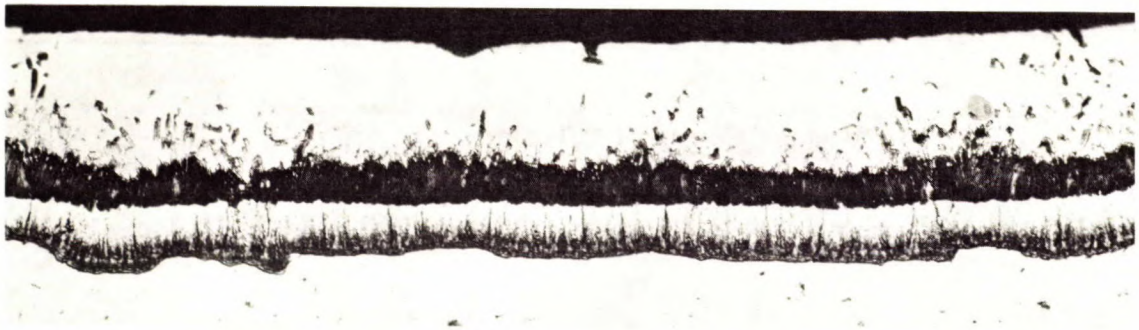

(a) Angle DA

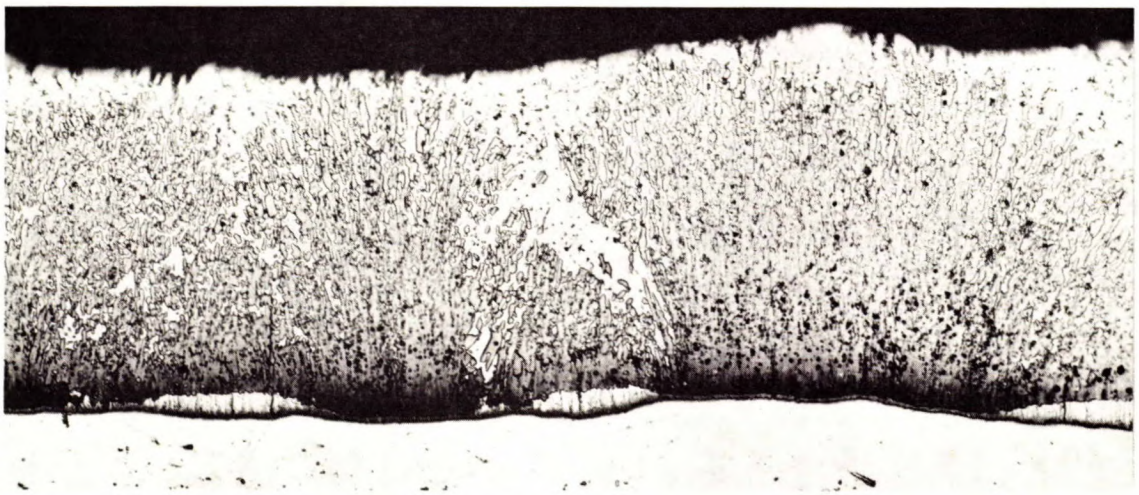

(b) Angle CA

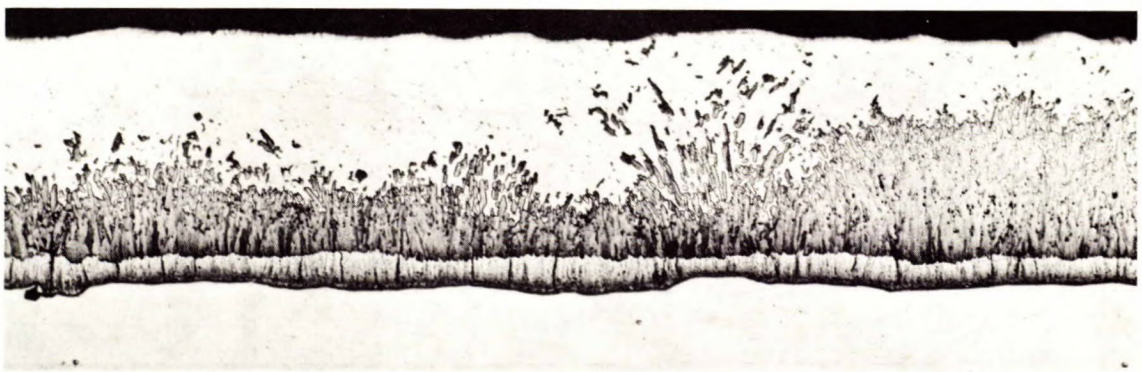

(c) Bar CB

Figure 3. As-galvanized coatings on angle and bar products. X250.

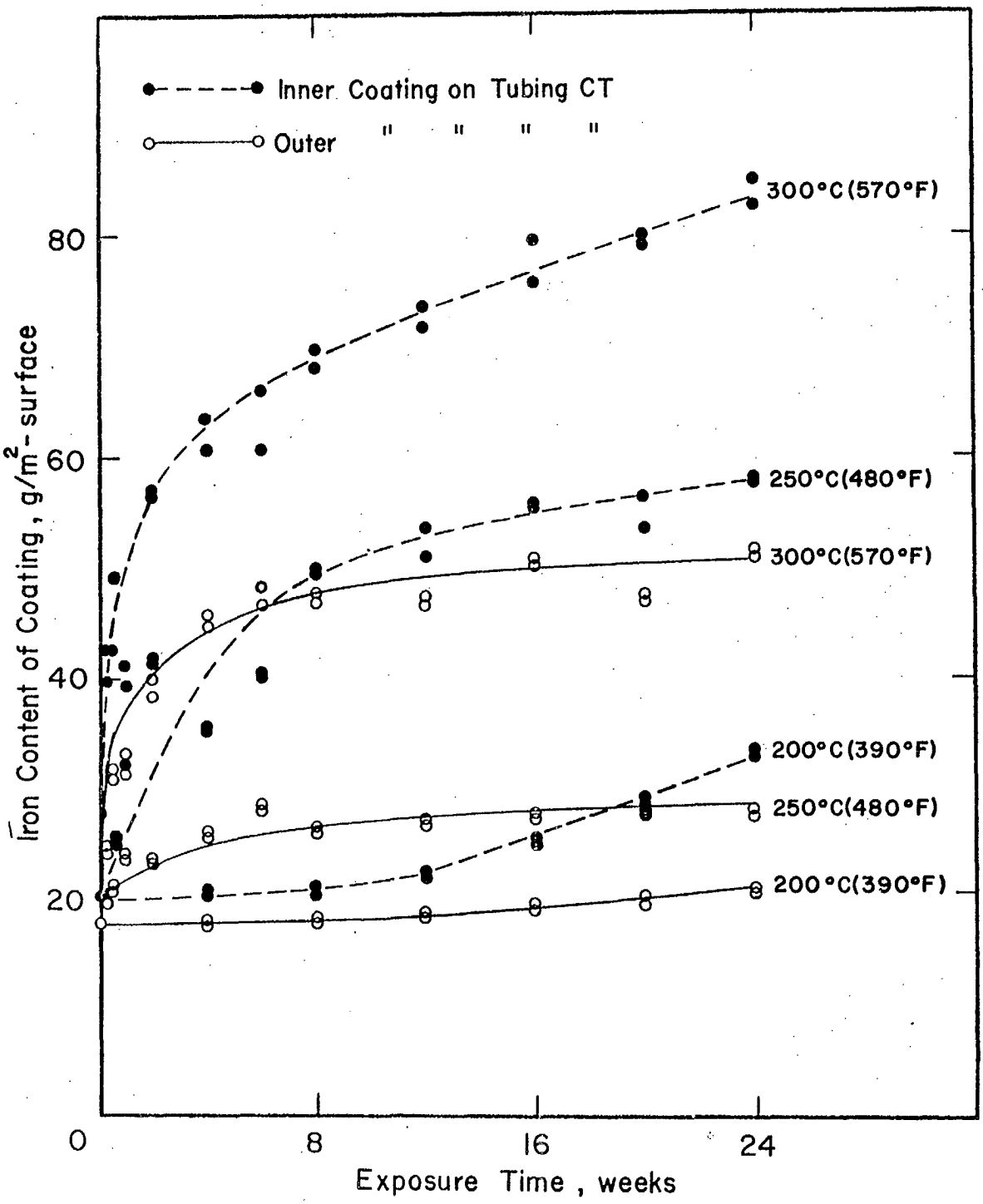

Figure 4. Effect of temperature and exposure time on iron content of coatings on Tubing CT.

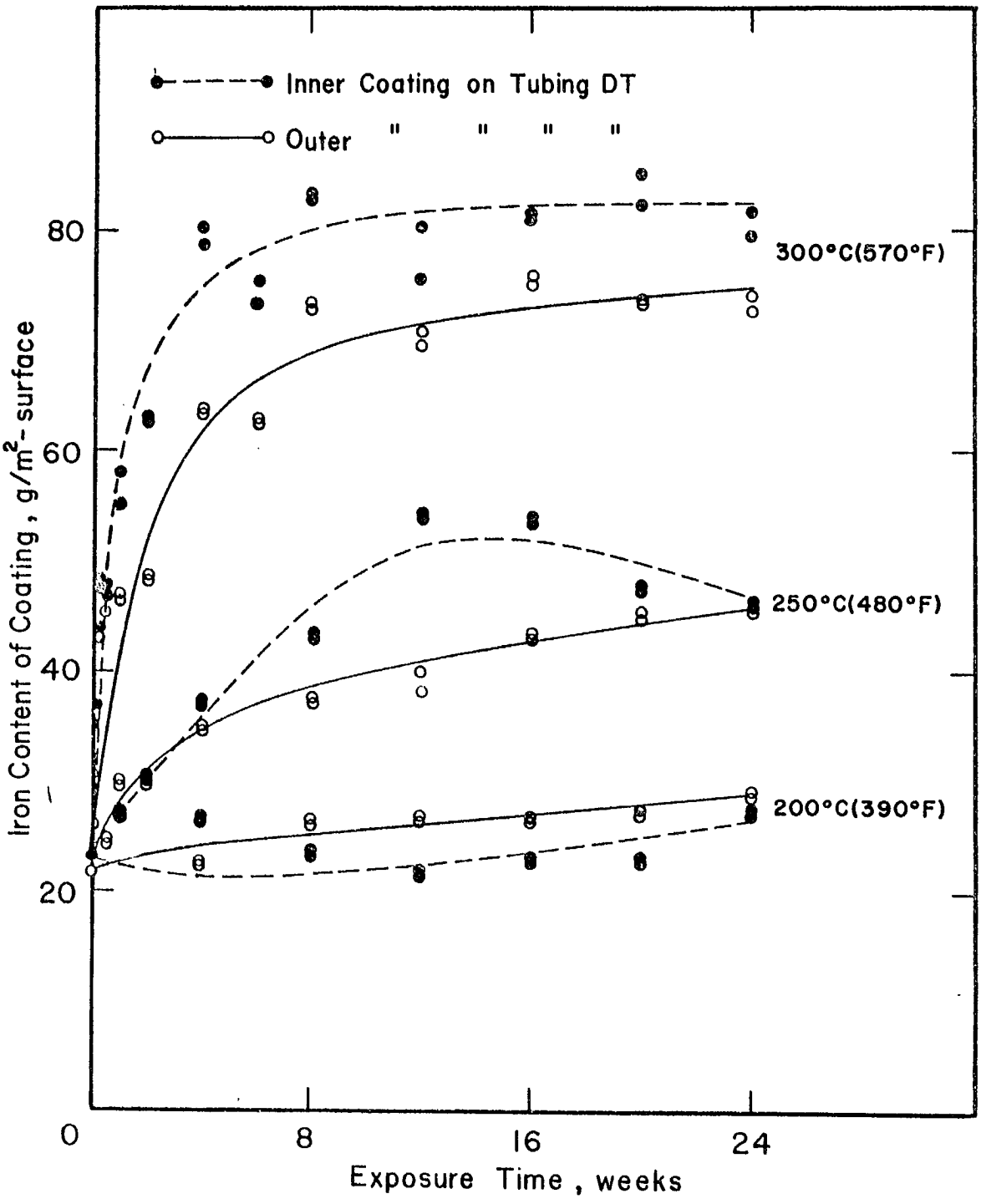

Figure 5. Effect of temperature and exposure time on iron content of coatings on Tubing DT.

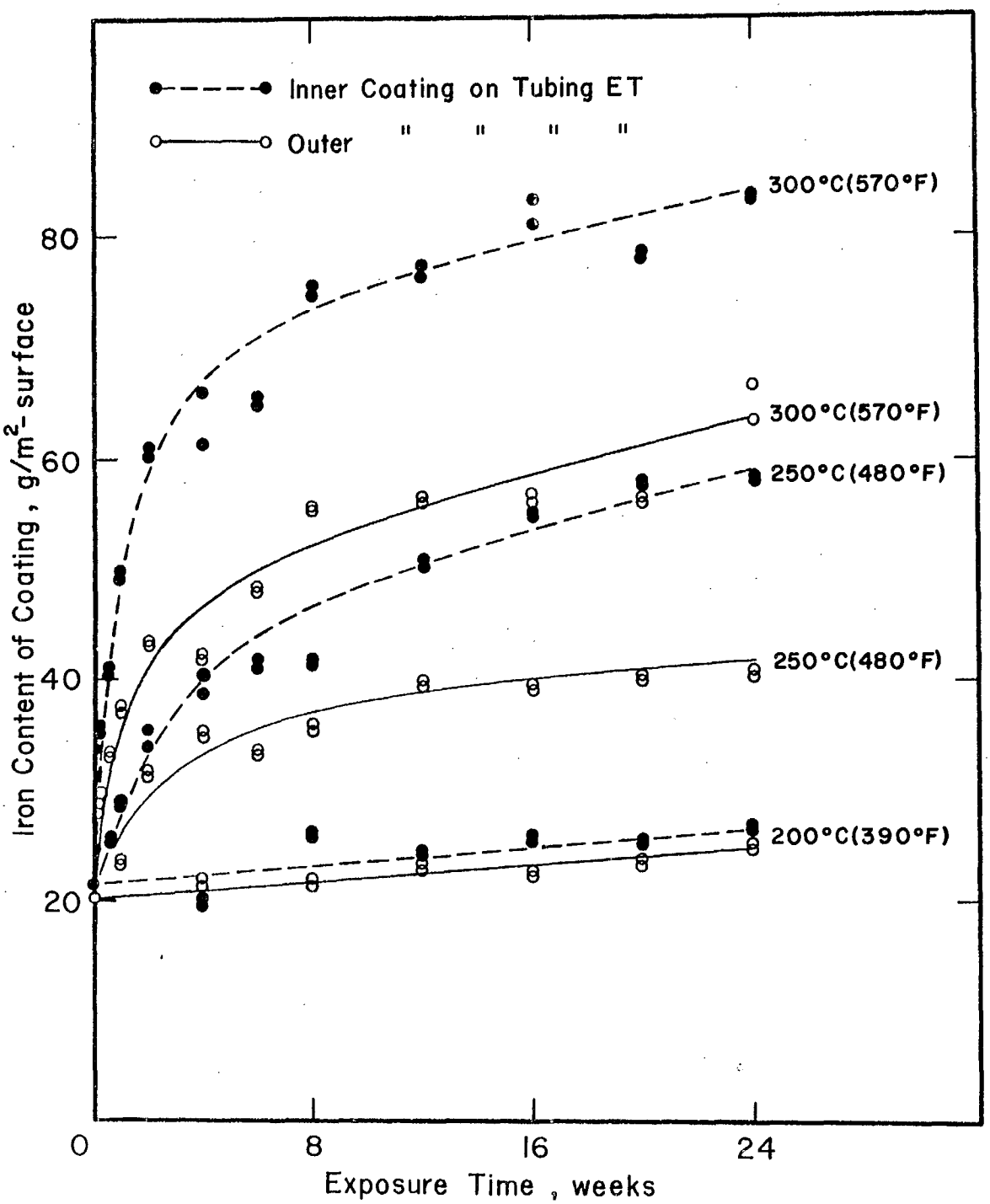

Figure 6. Effect of temperature and exposure time on iron content of coatings on Tubing ET.

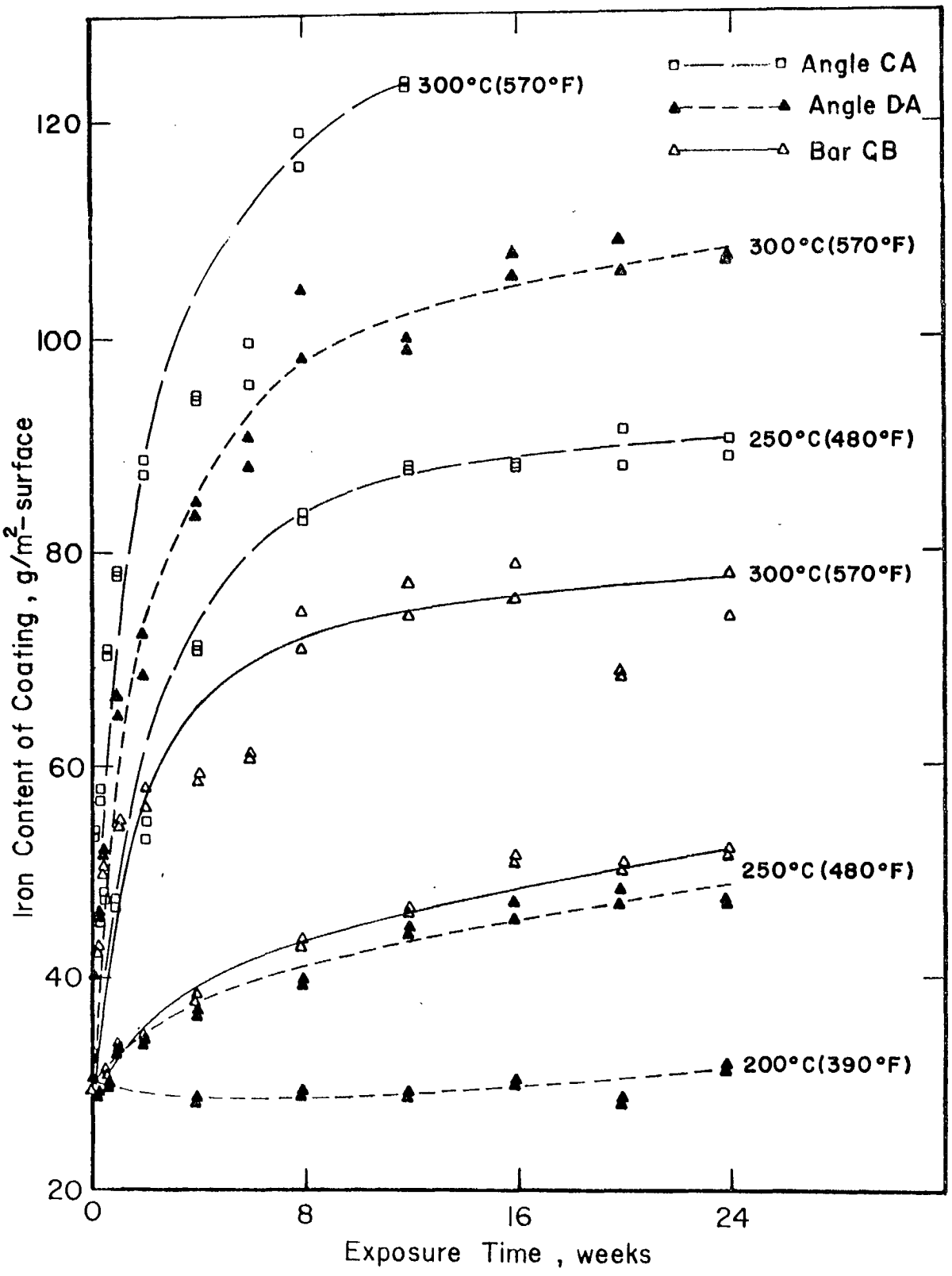

Figure 7. Effect of temperature and exposure time on iron content of coatings on Angles DA and CA, and Bar CB.

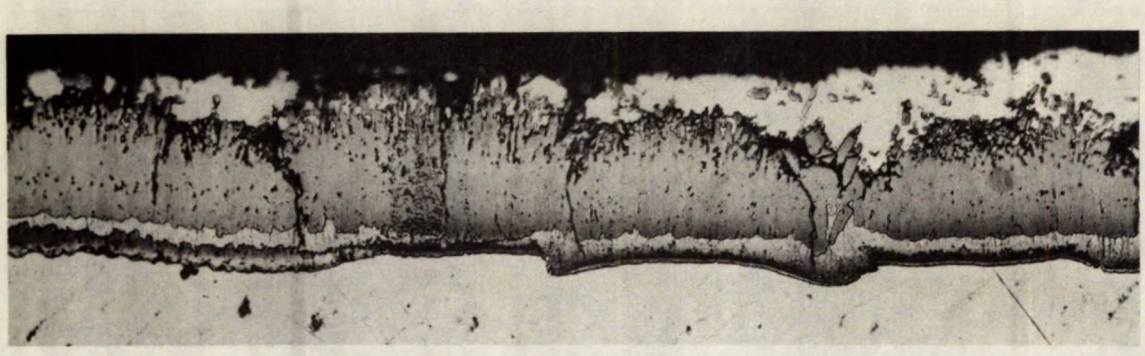

(a) CT (outer) - 16 wk

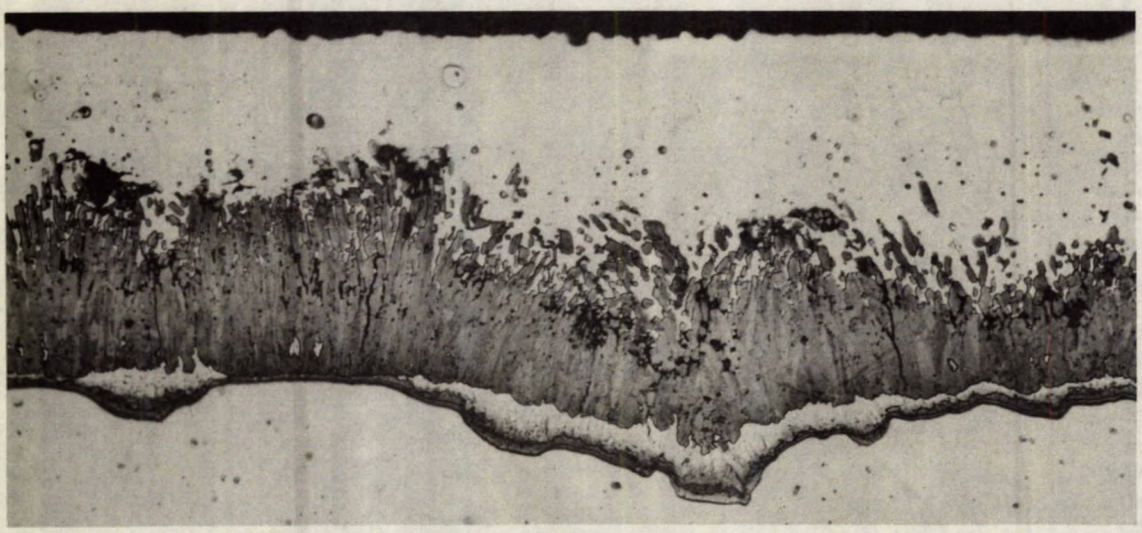

(b) CT (inner) - 16 wk

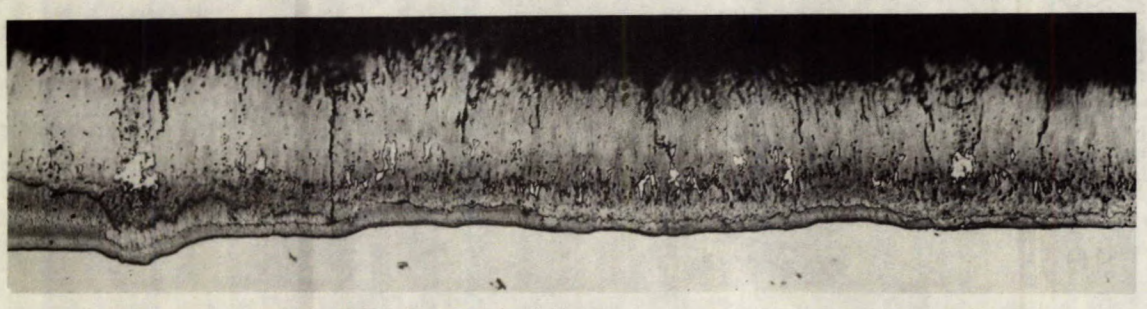

(c) CT (outer) - 1 yr

(d) CT (inner) - 1 yr

Figure 8. Coatings on Tubing CT heated at 200°C (390°F). X500.

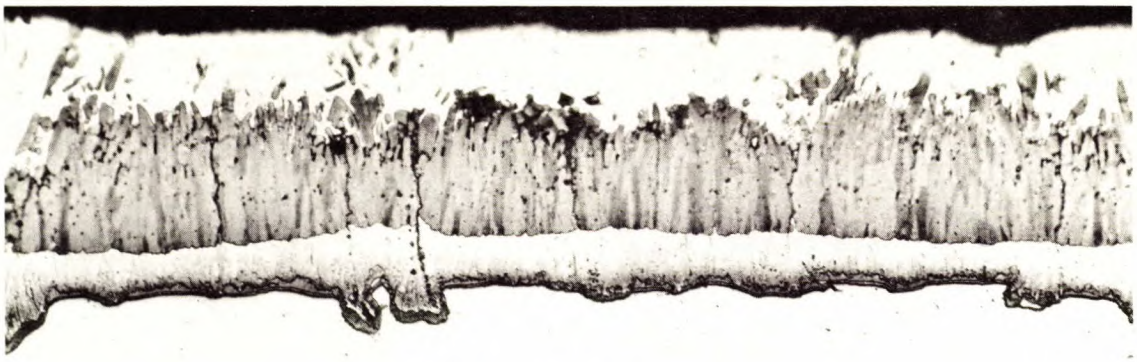

(a) DT - 24 wk

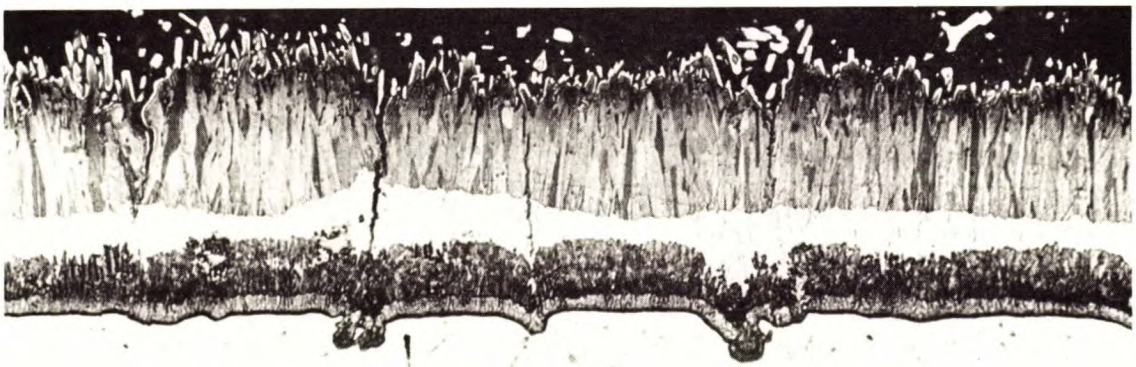

(b) DT - 1 yr

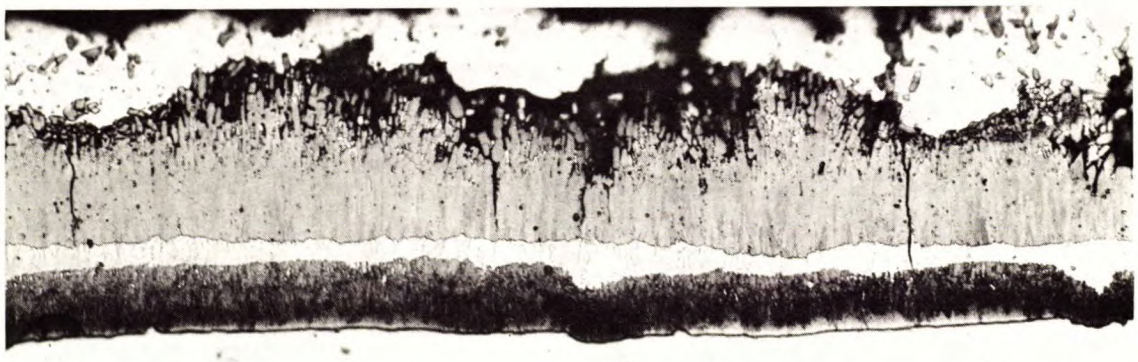

(c) ET - 24 wk

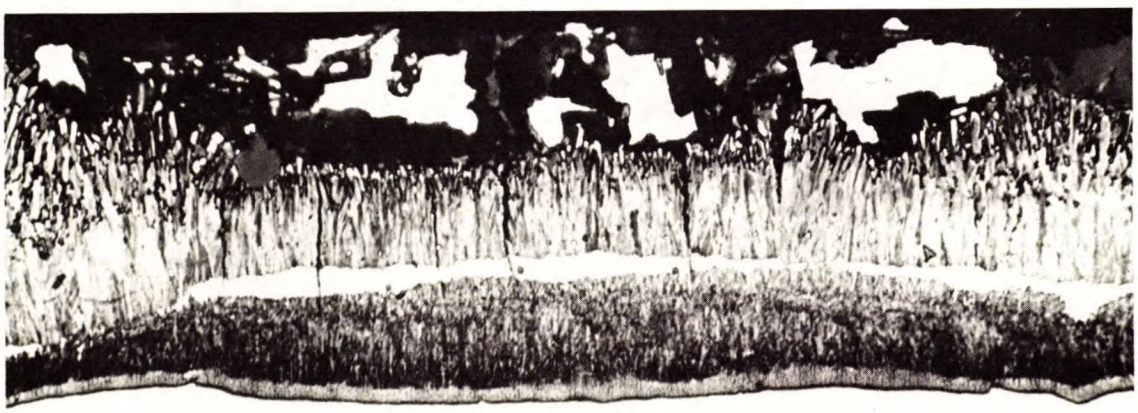

(d) ET - 1 yr

Figure 9. Outer coatings on Tubings DT and ET heated at 200°C (390°F). X500.

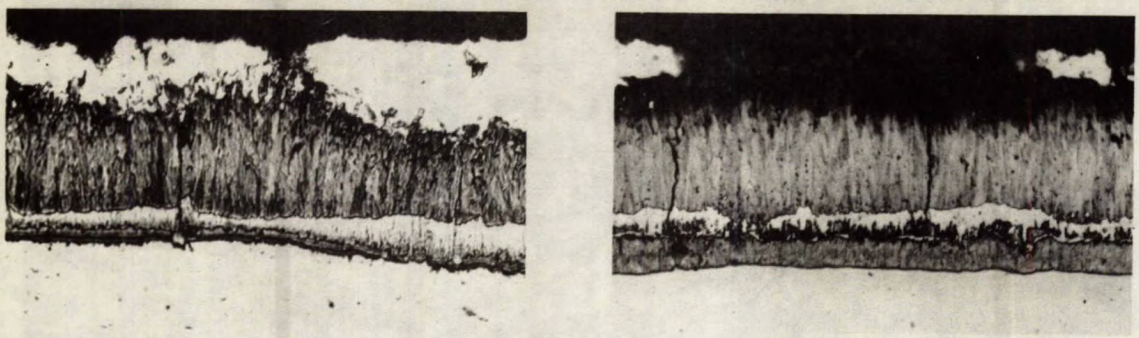

(a) 2 days CT (outer) (b) 2 wk

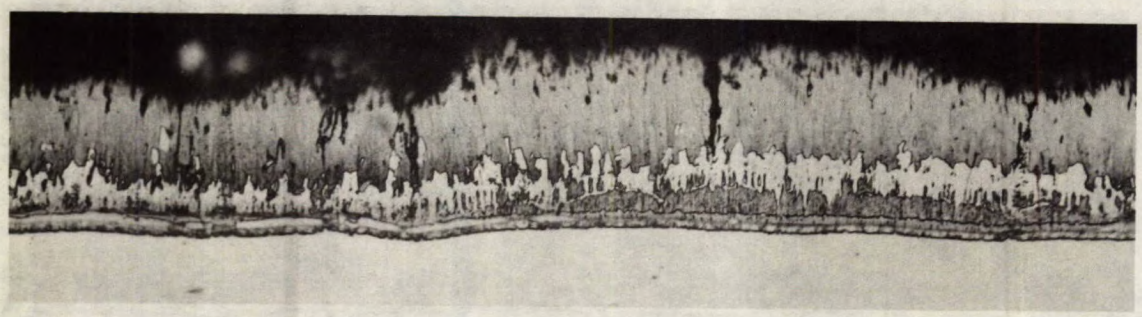

(c) CT (outer) - 24 wk

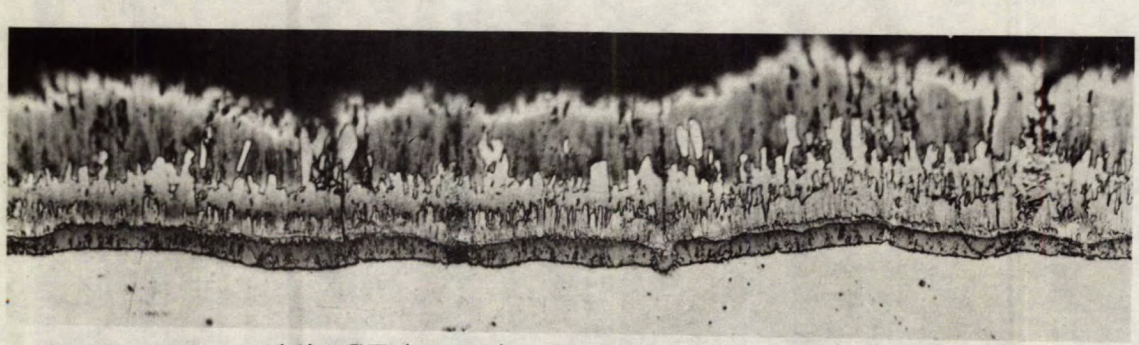

(d) CT (outer) - 1 yr

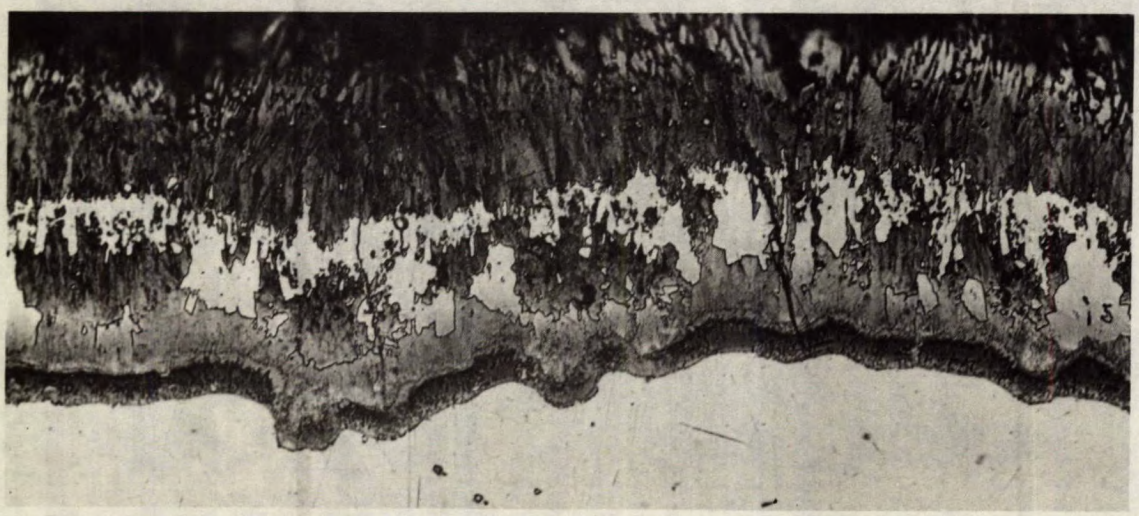

(e) CT (inner) - 1 yr

Figure 10. Coatings on Tubing CT heated at 250°C (480°F). X500.

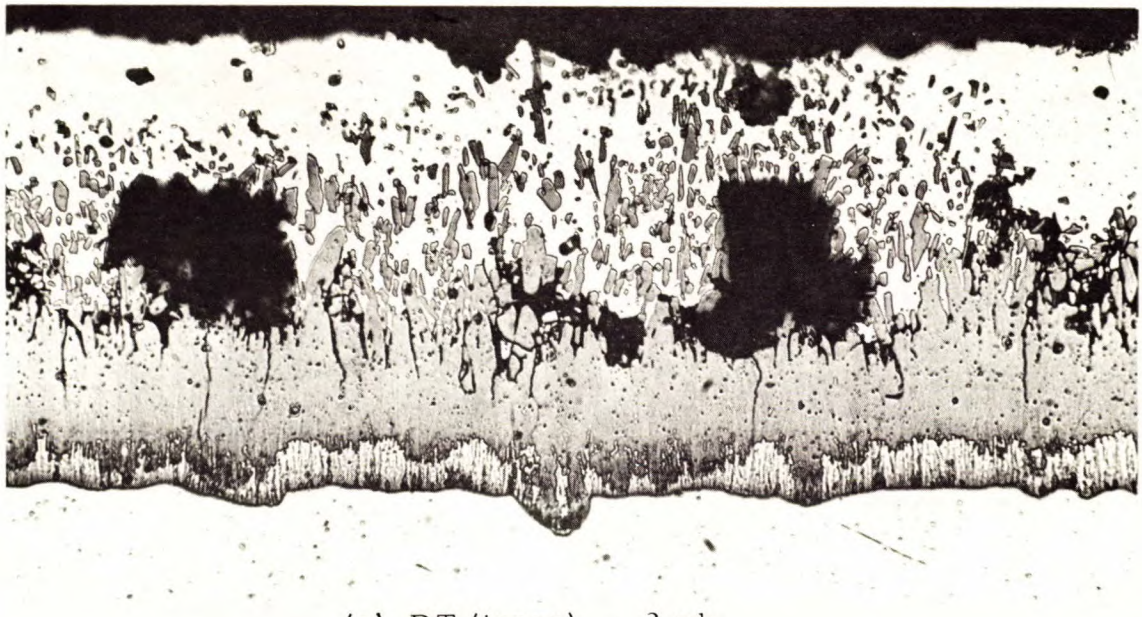

(a) DT (inner) - 2 wk

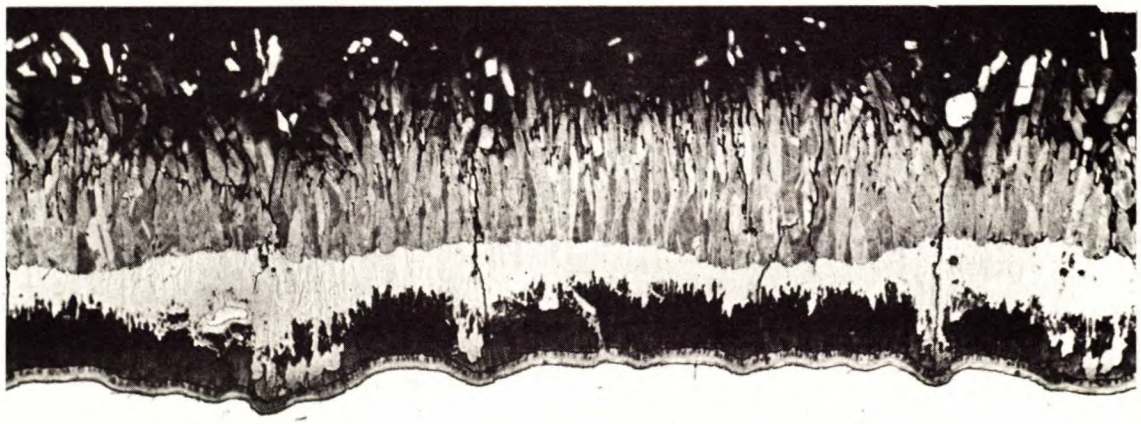

(b) DT (outer) - 20 wk

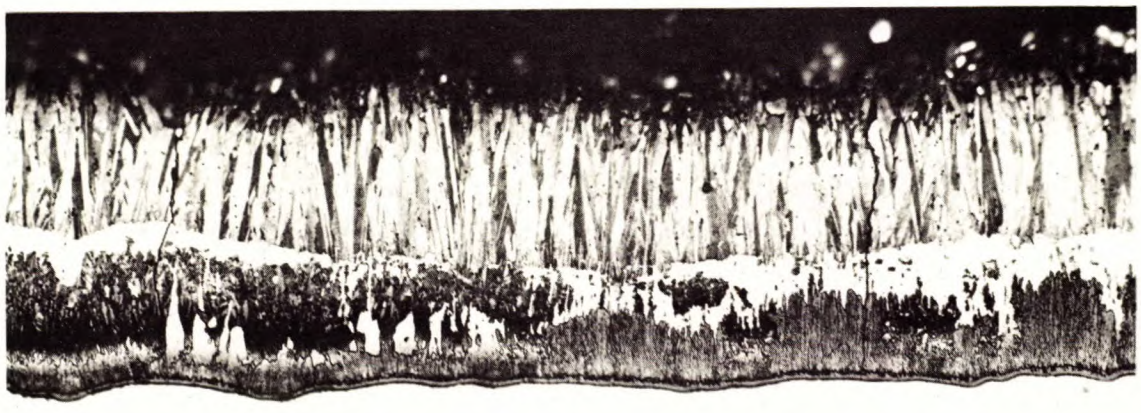

(c) DT (inner) - 24 wk

Figure 11. Coatings on Tubing DT heated at 250°C (480°F). X500.

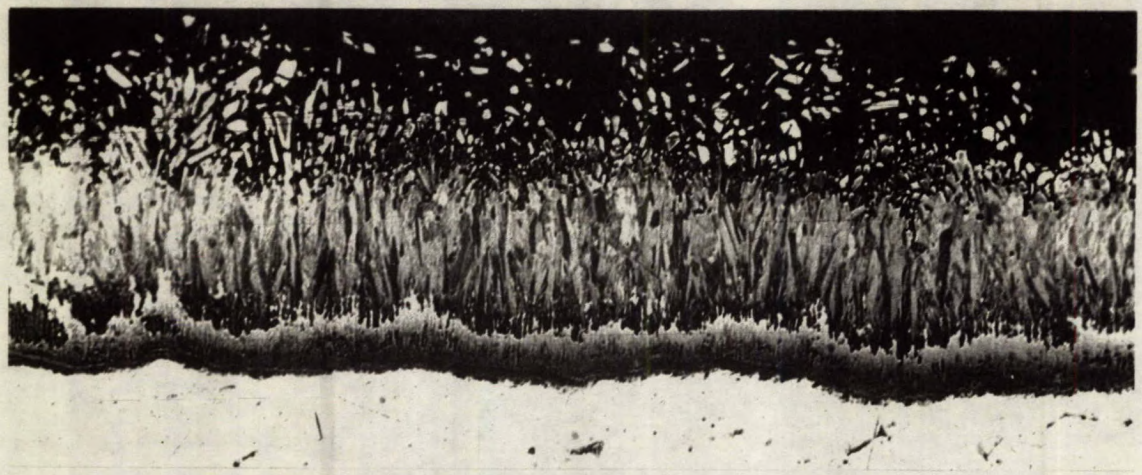

(a) ET (outer) - 24 wk

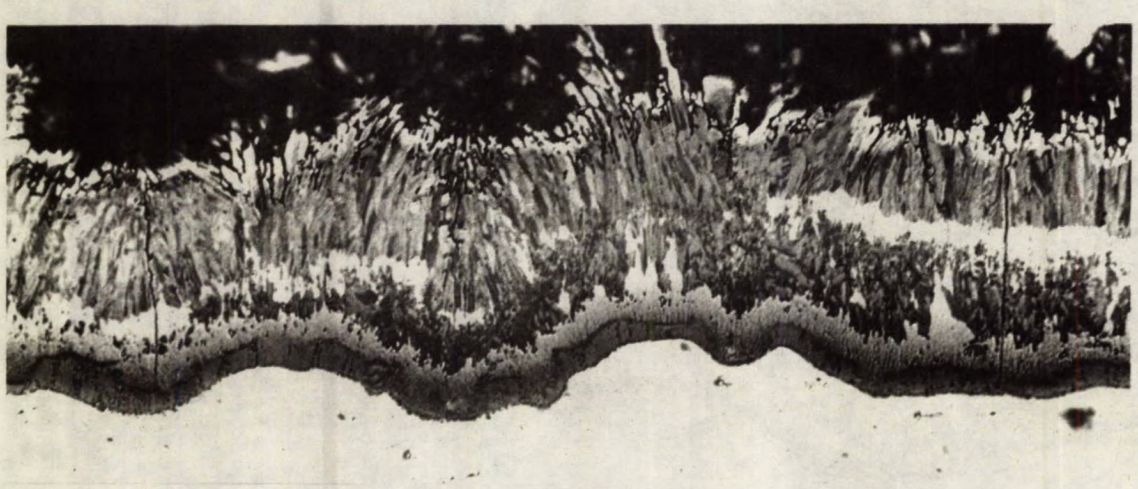

(b) ET (inner) - 24 wk

Figure 12. Coatings on Tubing ET heated at 250°C (480°F). X500.

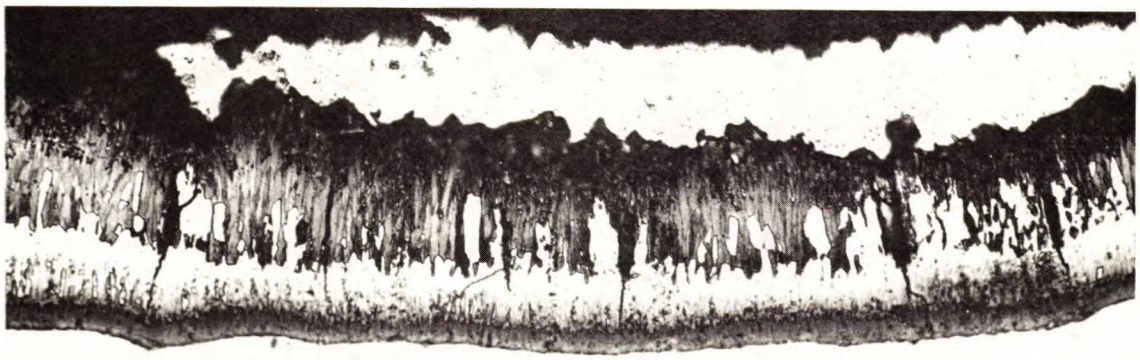

(a) CT - 2 wk

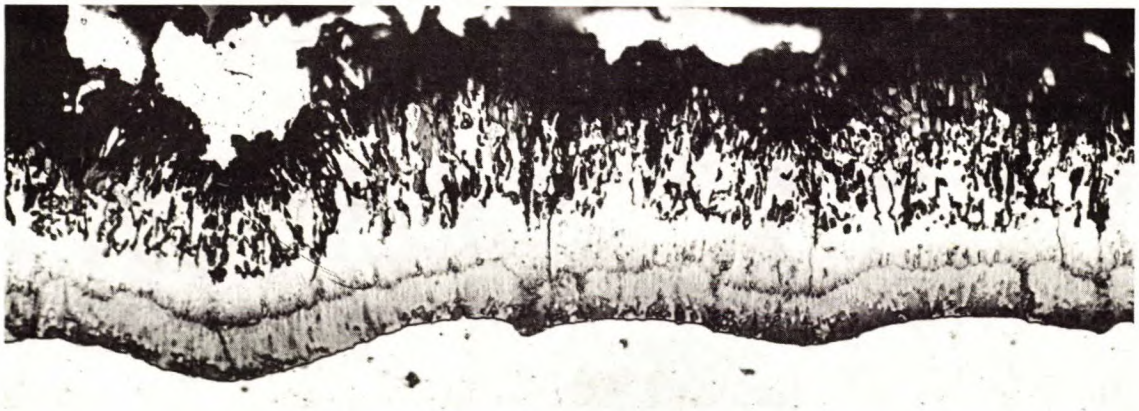

(b) CT - 4 wk

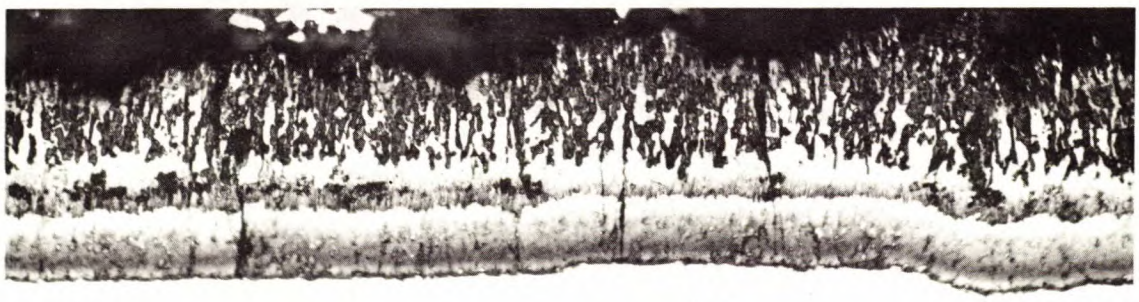

(c) CT - 16 wk

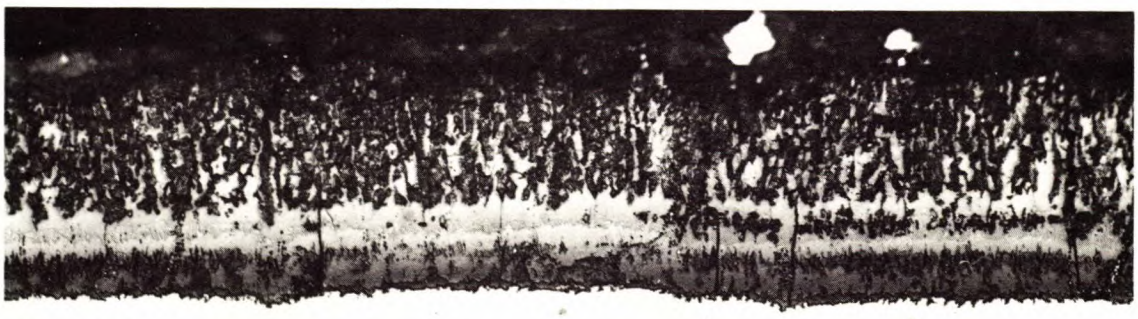

(d) CT - 24 wk

Figure 13. Outer coatings on Tubing CT heated at 300°C (570°F). X500.

(a) DT - 24 wk

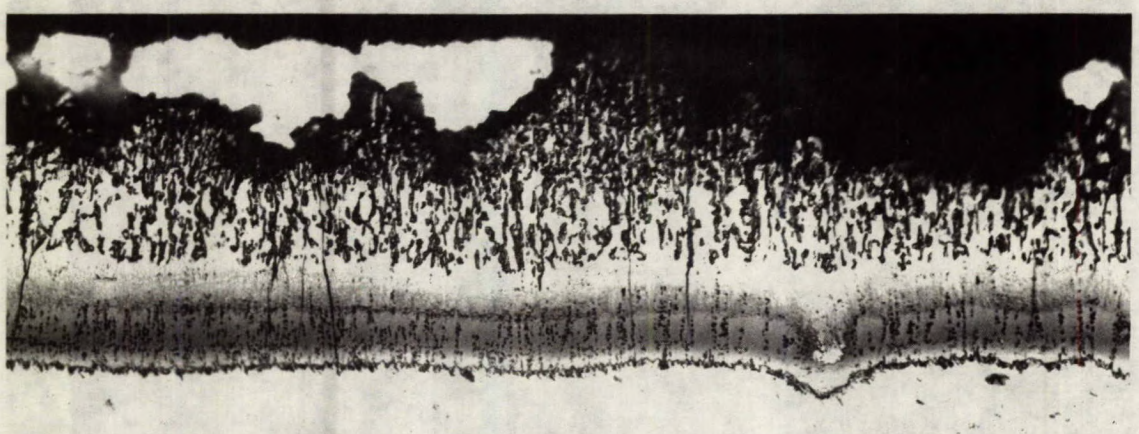

(b) ET - 24 wk

Figure 14. Outer coatings on Tubings DT and ET heated at 300°C (570°F). X500.

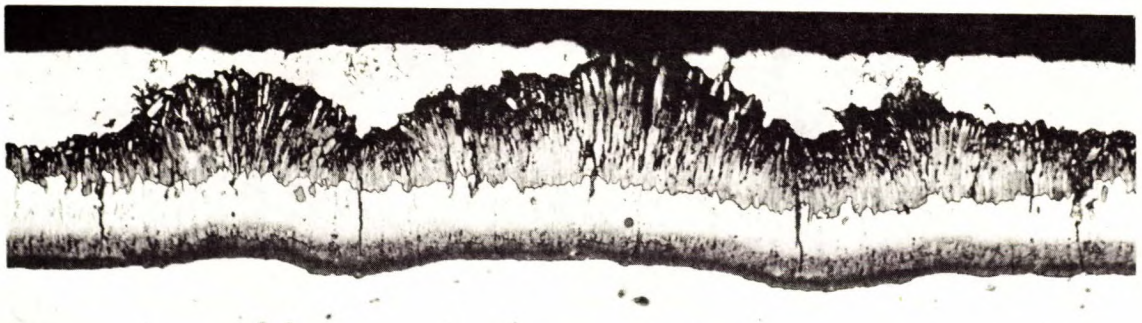

(a) CT - 1 hr

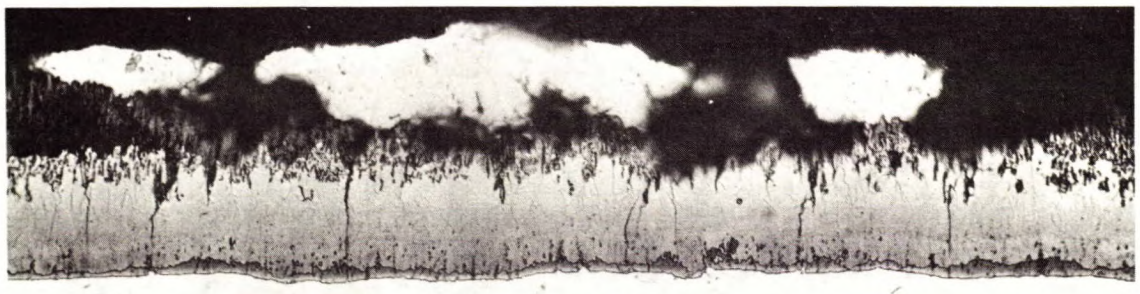

(b) CT - 2 hr

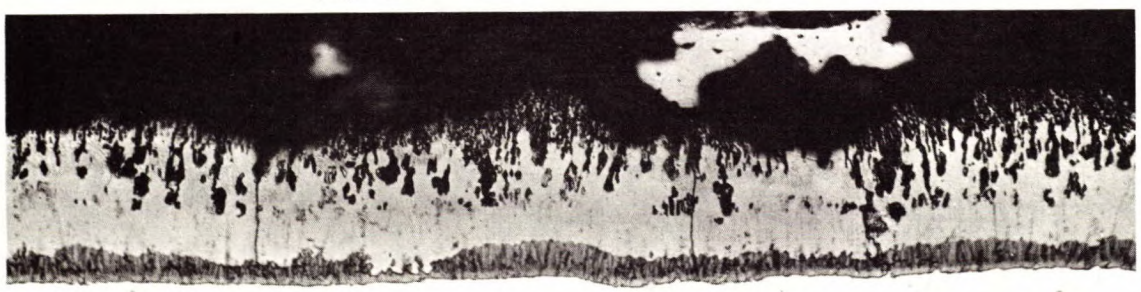

(c) CT - 16 hr

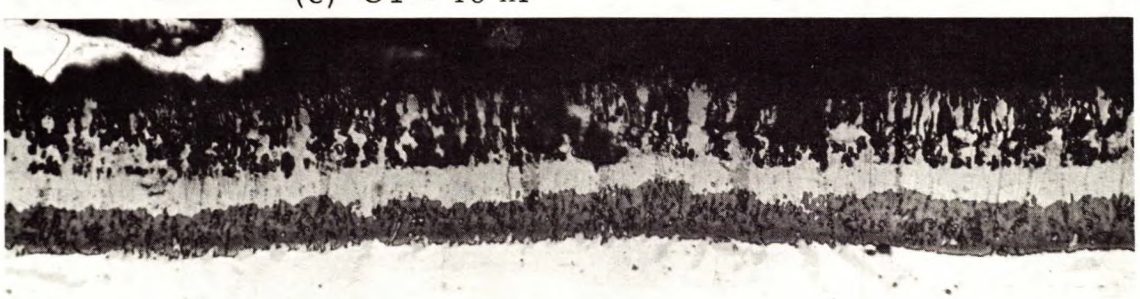

(d) CT - 2 wk

Figure 15. Outer coatings on Tubing CT heated at 400°C (750°F). X500.

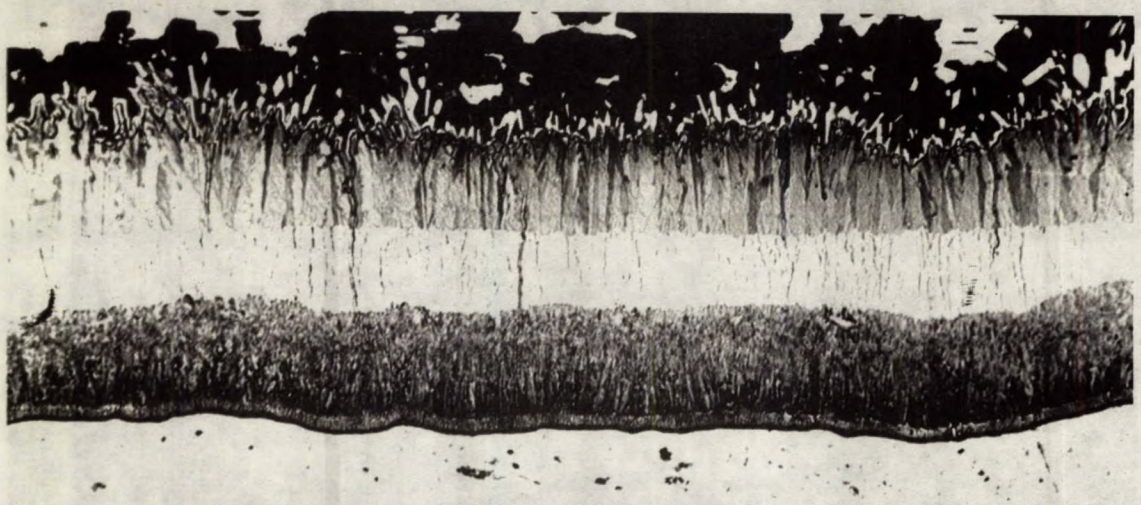

(a) DA - 1 yr at 200°C (390°F)

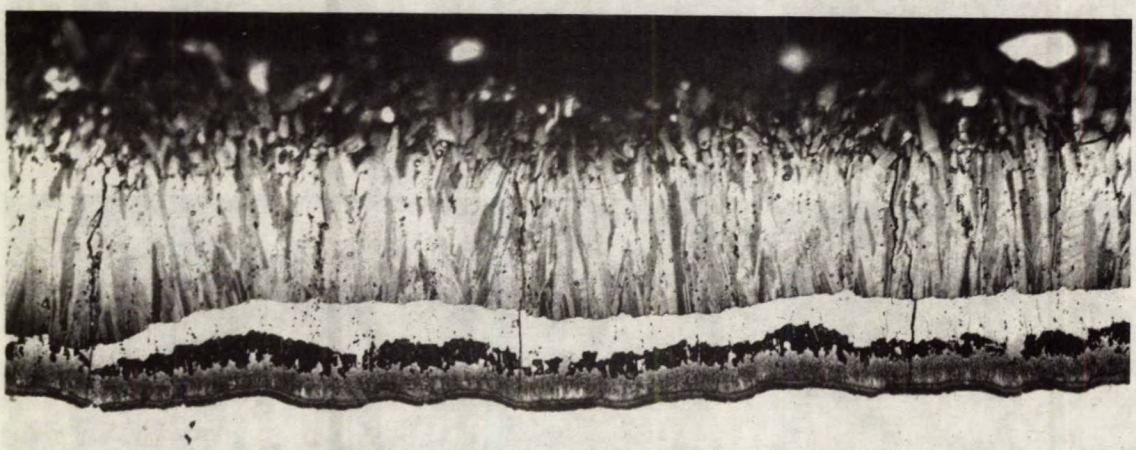

(b) DA - 24 wk at 250°C (480°F)

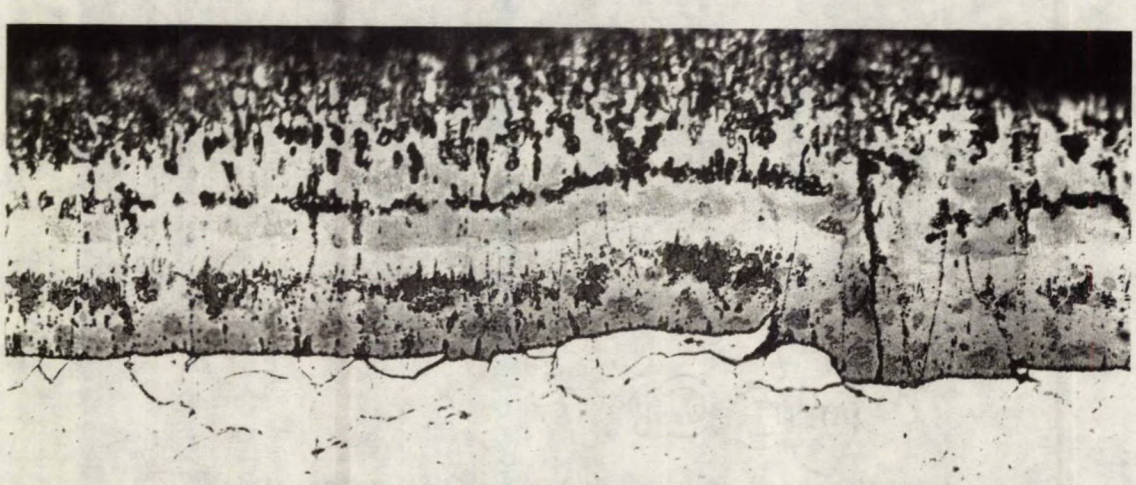

(c) DA - 24 wk at 300°C (570°F)

Figure 16. Coatings on Angle DA after exposure treatments indicated. X500.

(a) CA - 20 wk at 250°C (480°F)

(b) CA - 20 wk at 300°C (570°F)

Figure 17. Coatings on Angle CA after exposure treatments indicated. X250.
(Note lower magnification.)

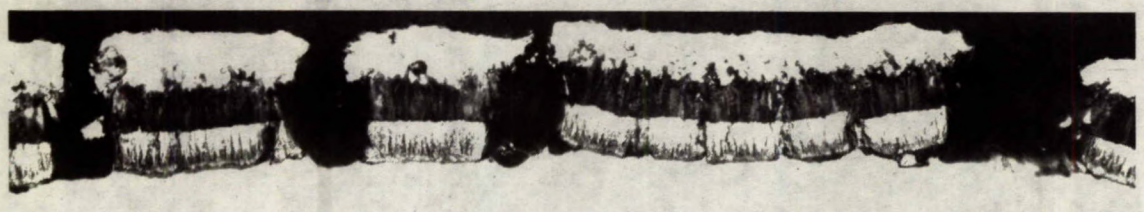

(a) as-galvanized

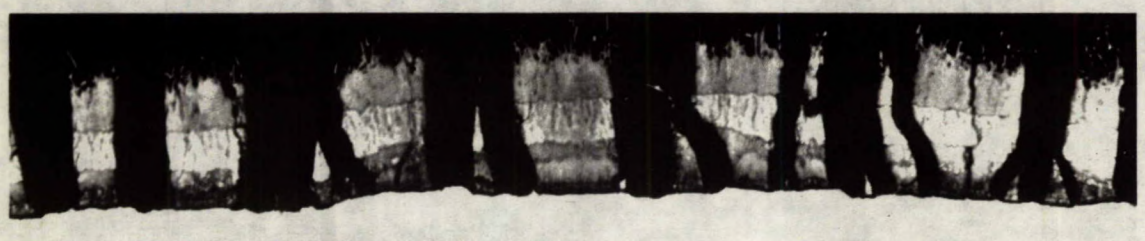

(b) 1 yr at 200°C (390°F)

(c) 24 wk at 300°C (570°F)

(d) 4 wk at 400°C (750°F)

Figure 18. Microstructures of as-galvanized and heat-treated samples of Angle DA after bending. X250.

====